Addis Ababa University

Addis Ababa Institute of Technology

School of Electrical and Computer Engineering

Performance Analysis and Investigation of Non-blind Adaptive Equalizers for Broadcasting Channels

By: Amare Tesfaw

Thesis Submitted To Addis Ababa Institute of Technology in Partial Fulfillment of the Requirements for the Degree of Master of Science in Electrical and Computer Engineering (Communication Engineering)

Advisor: Dr. -Ing. Dereje Hailemariam

October, 2017

Addis Ababa, Ethiopia

Addis Ababa University

Addis Ababa Institute of Technology

School of Electrical and Computer Engineering

Thesis Submitted To Addis Ababa Institute of Technology in Partial Fulfillment of the Requirement for the Degree of Master of Science in Electrical and Computer Engineering (Communication Engineering)

Performance Analysis and Investigation of Non-blind Adaptive Equalizers for Broadcasting Channels

By: Amare Tesfaw

Approval by Board of Examiners

______________________	__________	__________
Chairman, School Graduate Committee	Signature	Date
Dr. -Ing. Dereje Hailemariam	__________	__________
Advisor	Signature	Date
______________________	__________	__________
Internal Examiner	Signature	Date
______________________	__________	__________
External Examiner	Signature	Date

DECLARATION

I, the undersigned, declared that this MSc thesis is my original work, has not been presented for fulfillment of a degree in this or any other University and all sources and materials used for the thesis are duly acknowledged.

Amare Tesfaw ________________________

Name Signature

Addis Ababa ___________________________

Place Date of Submission

This thesis work has been submitted for examination with my approval as a University Advisor.

Dr. -Ing. Dereje Hailemariam _________________

Advisor's Name Signature

Acknowledgement

Next to God, this work was possible due to the guidance and support of many people. First of all, I would like to thank my advisor Dr.-Ing. Dereje Hailemariam, for his intellectual guidance and continuous encouragement. His patience and the time he invested in the whole process of this thesis work as well as his willingness to support me at any time helped me to bring this thesis in to fruition.

Secondly, I want to thank my families who have always been the sources of encouragement and strength throughout my life. I am also thankful for my friends in AAiT, for all the unforgettable moments we shared together.

I would also like to acknowledge Woldia University, for granting and sponsoring me for this scholarship program and finally, I must also acknowledge Ethiopian Information Network Security Agency (INSA) for raising this research idea and partially funding my thesis.

Abstract

Adaptive equalization is a process of compensating the disruptive effects caused by inter symbol interference (ISI) in a band limited channel and plays a vital role for enabling higher data rate transmissions in digital communication systems. In this thesis, different linear and non-linear non-blind equalization techniques were studied to select the appropriate technique to be applied in frequency selective broadcasting channels. The study is part of a joint project between Information Networks Security Agency (INSA) of Ethiopia and Addis Ababa University (AAU) that intends to implement advanced digital receiver with adaptive equalizer for a certain application in broadcasting systems.

For simulation test, Recursive Least Square (RLS) algorithm based linear equalizer was implemented in MATLAB software. Using this equalizer, it was possible to recover a corrupted image signal successfully after passing through a frequency selective fading channel modeled as typically urban (TU) model with 6 signal paths. Performance of the RLS equalizer in training only and decision directed training modes were also compared and simulation results show that the RLS equalizer in decision directed training mode performs better than the same equalizer in training only mode. Therefore, based on the results obtained, the RLS equalizer in decision directed training mode is recommend for implementation by the industry.

Keywords: *Adaptive Equalizer, Frequency Selective Channel, Adaptive Algorithms, LMS Algorithm, RLS Algorithm, Broadcast Channels, TU6 Channel Model.*

Table of Contents

List of Tables

List of Figures

List of Abbreviations

AAU	Addis Ababa University
AM	Amplitude Modulation
ATSC	Advanced Television Systems Committee
AWGN	Additive White Gaussian Noise
BCH	Bose-Chaudhuri-Hocquenghem
BEM	Basis Expansion Model
BER	Bit Error Rate
BPSK	Binary Phase Shift Keying
BU	Bad Urban
CD3	Coded Decision Directed Demodulation
CDM	Companded Delta Modulation
CEDS	Conventional Euclidean Direction Search
CE-BEM	Complex Exponential Basis Expansion Model
COFDM	Coded Orthogonal Frequency Modulation
COST	Cooperation in Science and Technology
CMA	Constant Modulus Algorithm
DAB	Digital Audio Broadcasting
DFE	Decision Feedback Equalizer
DRM	Digital Radio Mondiale
DVB	Digital Video Broadcasting

DVB-C	Digital Video Broadcasting- Cable
DVB-H	Digital Video Broadcasting- Handheld
DVB -T	Digital Video Broadcasting-Terrestrial
DVB-S	Digital Video Broadcasting- Satellite
FEDS	Fast Euclidean Direction Search
FIR	Finite Impulse Response
FM	Frequency Modulation
HE AAC V2	High Efficiency Advanced Audio Coding Version 2
HD	High Definition
HT	Hilly Terrain
INSA	Information Networks Security Agency
IIR	Infinite Impulse Response
ISDB	Integrated Services Digital Broadcasting
ISDB-C	Integrated Services Digital Broadcasting-Cable
ISDB-T	Integrated Services Digital Broadcasting Terrestrial
ISDB-Tsb	Integrated Services Digital Broadcasting–Terrestrial sound broadcasting
ISDB-S	Integrated Services Digital Broadcasting-Satellite
ISI	Inter-Symbol Interference
ITU	International Telecommunication Union
LDPC	Low Density Parity Check
LMS	Least Mean Squared Algorithm

LOS	Line-of-Sight
ML	Maximum Likelihood
MLSE	Maximum Likelihood Sequence Estimation
MMSE	Minimum Mean Squared Error
MPEG	Moving Picture Experts Group
OEDS	Optimal Euclidean Direction Search
OFDM	Orthogonal Frequency Division Modulation
PDF	Probability Density Function
PSK	Phase Shift Keying
QAM	Quadrature Amplitude Modulation
QPSK	Quadrature Phase Shift Keying
RA	Rural Area
RC	Raised Cosine
REDS	Recursive Euclidean Direction Search
RLS	Recursive Least Squared Algorithm
SBS	Symbol by Symbol
SE	Sequence Estimator
SGA	Stochastic Gradient Algorithm
SHOSS	Second and Higher Order Signal Statics
SNR	Signal to Noise Ratio
SRRC	Square Root Raised Cosine

TU	Typical Urban
USA	United States of America
US	Uncorrelated Scattering
VSB	Vestigial Sideband Modulation
WAVE	Wireless Access in Vehicular Environment
WiMAX	Worldwide Interoperability for Microwave Access
WSS	Wide Sense Stationary
WSSUS	Wide Sense Stationary Uncorrelated Scattering
ZF	Zero Forcing

Chapter One

Introduction

1.1 Background

Communications of wireless systems in terrestrial environments such as mobile and broadcasting systems mainly rely on multiple copies of a transmitted signal arriving at the receiver through multiple paths. The existing terrestrial effects lead to multi-path propagation (as free space transmissions rarely occur) which in turn affects quality of communication [1].

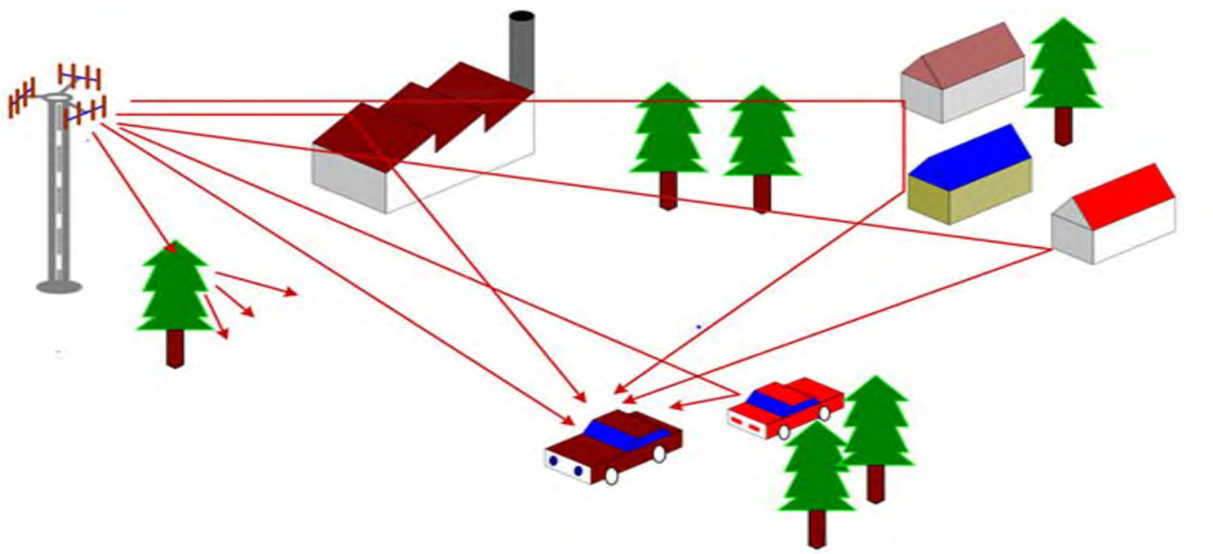

Figure 1.1: Multi-path transmission in a broadcasting application [1]

As shown in Figure 1.1 above, there are three basic mechanisms that impact signal propagation in wireless communication systems. This are: *reflection*, *diffraction*, and *scattering*. Because of these mechanisms, the transmitted signal generally propagates to the receiver antenna through many different paths. Thus, due to reflectors and scatterers (e.g., as cars, buildings and trees), the receiver antenna will receive multiple, delayed and scaled copies of the transmitted signal. These signals with different arrival time and phase may add constructively to yield undistorted signal or destructively, to yield a faded signal [2]. As a result, a particular signal path components arriving with various attenuations and delays are combined at the receiver. The delayed components can be considered as echoes that cause time dispersion of the transmitted signal. If time dispersion is greater than a substantial fraction of the signaling period, the channel responses to the subsequent data signals overlap. This effect is known as *inter-symbol interference* (ISI). Thus, the signal observed at the receiver input contains information on a certain number of data signals simultaneously.

In many cases the channel impulse response spans tens of signaling periods and ISI appears to be a major impairment introduced by the channel [3]. This destructive influence of ISI on a digital communication system performance has to be counteracted by special receiver and/or transmitter design. The part of the receiver that counteracts ISI is called *channel equalizer*.

Very often transmission channel characteristics are either not known at the beginning of a data transmission session or they are time variant. Therefore, it is advantageous to make the equalizer adaptive such that it can compensate for the distorting channel characteristics and simultaneously track the changes of channel characteristics in time [3]. In order to do that successfully, the equalizer needs to guess or estimate the response of the channel being used. Based on the requirements of additional information about the transmitted signal over the random channel, equalizers can be categorized into three groups; namely, non-blind, blind and semi-blind equalizers.

The first case is non-blind equalizer which requires an initial training period, during which a known data sequence is transmitted and a replica of this sequence is made available at the receiver in proper synchronism with the transmitter. This mechanism makes it possible for adjustments to be made to the equalizer coefficients in accordance with the adaptive filtering algorithm employed in the equalizer design [4], [5]. Zero forcing (ZF), minimum mean squared error (MMSE), least mean square (LMS), recursive least square (RLS), decision feedback equalizer (DFE) and maximum likelihood sequence estimation (MLSE) based equalizers are included in this category.

These techniques simplify the receiver design, reduce the computational load and can be quite easily applied in wireless communications [5]. Although they may impose unnecessary overhead that could limit the effective data throughput, they outperform the blind and semi-blind equalization schemes in time-varying channels. Because of those performance issues and the needs of the sponsor industry, training-based equalizers are chosen to be the main focuses of this thesis work.

On the other hand there is also a case in which the receiver tries to compensate the effect of the channel without the need for the knowledge of the desired output (or training signal). In this case the receiver has to be intelligent enough to recover a known property of the signal from a received corrupted signal. This type of equalization technique is called *blind equalization*. The constant modulus algorithm (CMA) is the most widely used blind equalization algorithm. Stochastic gradient algorithm (SGA), maximum likelihood (ML) and second and higher order signal statics (SHOSS) based equalizers are also included in this category. They are particularly suitable for applications where the bandwidth is a scarce resource. However, they are computationally intensive and, hence, not appropriate for real-time implementations in complex time-varying systems or for low cost receivers [6], [5].

The third types of equalizers are called semi-blind equalizers and they try to fill the gaps between training-based and blind equalization techniques. In this case, blind methods are used together with training symbols in order to improve the drawbacks of both methods. These methods transmit known training or pilot symbols at the beginning of each frame for synchronization and initial channel estimation, and then feed the detected symbols back to the channel estimator updating the earlier estimate. They are computationally less complex than that of blind equalization techniques; however, their performance is not comparable to training-based channel equalizers [8]. Euclidean direction search (EDS) algorithm based equalizers such as, conventional Euclidean direction search (CEDS), fast Euclidean direction search (FEDS), recursive Euclidean direction search (REDS) and optimal Euclidean direction search (OEDS) algorithms are under the category of semi-blind equalizers [1], [7].

1.2 Overview of Digital Broadcast Systems

Digital broadcasting is the practice of using digital signals rather than analogue signals for broadcasting audio/video signals over radio-frequency bands. In this section overview of digital radio and television broadcasting systems are discussed briefly.

1.2.1 Digital Radio Broadcasting Systems

Different digital terrestrial broadcasting systems have been proposed for the delivery of radio content over the last 20 years. The three most important systems being implemented or already in operation are briefly outlined in the following subsections.

Digital Audio Broadcasting (DAB) Family: Terrestrial-digital audio broadcasting (T-DAB) has been standardized in 1997 and rests on four basic pillars, namely an appropriate source coding technology (moving picture experts group (MPEG) layer I, layer II also known as MUSICAM), special channel coding algorithms (punctured convolutional codes), multiplexing of several programs, and coded orthogonal frequency division modulation (COFDM) as the modulation scheme for signal transmission. However, the source coding techniques are outdated in recent times and an enhancement of T-DAB called *DAB+* was standardized in 2007. In this standard MUSICAM was substituted by high efficiency advanced audio coding version 2 (HE AAC v2) which allows higher data reduction rates compared to T-DAB and the channel coding has been enhanced by Reed-Solomon coding in order to make the transmission more robust [8].

Digital Radio Mondiale (DRM): It is a COFDM system like T-DAB. According to the standard DRM can be used below 30 MHz in short and medium wave regime which is meant to substitute the analogue amplitude modulation (AM) transmissions. Therefore, it employs a bandwidth of 9 or 10 kHz only. Compared to the T-DAB family, this is very narrowband. However, such a bandwidth has been chosen to fit DRM into the existing AM channel raster [8].

High Definition (HD) Radio: In United States of America (USA), a proprietary standard for a digital terrestrial radio broadcasting system, called *HD Radio*, has been developed. It is also COFDM system which can be employed in the AM and frequency modulation (FM) bands. The development was governed by the intention to support simultaneous operation of legacy analogue services, while allowing for gradual transition to digital services. The basic idea of HD Radio is to transmit one or two digital signals alongside with an analogue AM or FM signal [8].

1.2.2 Digital Television Broadcasting Systems

Several digital terrestrial broadcasting systems for the distribution of television services have been developed and rolled-out in different parts of the world. For example, the Integrated Service Digital Broadcasting (ISDB) system is standard in Japan while Advanced Television Systems Committee (ATSC) is the main standard in USA. Also the Digital Video Broadcasting (DVB) standard is most widespread in Europe. These systems are briefly introduced below.

DVB standards: DVB is the agency responsible for creating and submitting standardization procedures for digital television broadcasting systems. The following DVB techniques have been defined in the standard: Digital Video Broadcasting -Cable (DVB-C), adopted in 1994, Digital Video Broadcasting -Satellite (DVB-S), in 1995, and DVB-T, in 1997. DVB has also developed the DVB-T standard for handheld devices, named Digital Video Broadcasting - Handheld (DVB-H). With the joint use of orthogonal frequency division modulation (OFDM) and channel coding, the main problems of analog television, such as poor use of the spectrum and noise effects, are solved in these standards. Subsequently, enhanced versions of these systems, such as DVB-C2, DVB-S2, DVB-T2 or DVB-SH, have been developed due to the need for new services that require greater capacity [8].

ATSC: The ATSC group helped in developing the new digital television standard for USA. Several other countries such as Canada, Korea and Mexico have adapted to this standard. The ATSC standard also includes terrestrial, cable and satellite transmissions. For terrestrial use, the 8- vestigial sideband modulation (VSB) modulation form is applied. When cable is used the signal to noise ratio (SNR) is higher, and more advanced forms of modulation can be used, such as 16- VSB and 256-quadrature amplitude modulation (256-QAM), to capsule more information on the same channel bandwidth. The modulation forms used in the satellite standard are quadrature phase shift keying (QPSK), 8PSK and 16QAM [8].

ISDB: ISDB standard was created to transmit signals from television stations in the new digital format. It includes Integrated Service Digital Broadcasting-Satellite (ISDB-S), Integrated Service Digital Broadcasting-Terrestrial (ISDB-T), Integrated Service Digital Broadcasting-Cable (ISDB-C), Integrated Service Digital Broadcasting-Terrestrial sound broadcasting (ISDB-Tsb) and a mobile broadcasting standards for the 2.6 GHz band.

Compression of video and audio in ISDB is done with MPEG-2. ISDB is split up in different modulations, due to different requirements of different frequency bands and media. PSK-modulation is used in ISDB-S for the 12 GHz band. Companded delta modulation (CDM) is used in the 2.6 GHz band for ISDB-Tsb and COFDM modulation with PSK/QAM in ISDB-T [8].

1.3 Statement of the Problem

The biggest challenges in modern wireless communication systems are signal fading and ISI introduced by random and time-varying channel. Due to multipath propagation and mobility of the channel and the receiver, many copies of a transmitted signal arrive at the receiver antenna at different instants with different attenuation and delay characteristics. When these delayed signal components are separated by more than a symbol duration, ISI results. Therefore, as a result of these distortions, wireless fading channels show dramatically poorer Bit Error Rate (BER) performance than traditional Additive White Gaussian Noise (AWGN) channels. To mitigate this challenging problem, wireless communication system designers employ digital channel equalizers that can minimize those undesired and destructive ISI effects.

The idea of studying these channel equalizers was first initiated as a result of interests from Information Networks Security Agency (INSA) of Ethiopia to implement effective digital receivers with adaptive equalizers. To achieve that, the industry is working with Addis Ababa University (AAU) on an industrial project that aims to implement optimal non-blind adaptive equalizers to mitigate ISI effects for a certain digital broadcasting application. Hence, the motivation of the thesis is identifying an optimal non-blind adaptive equalization method to mitigate ISI for broadcasting system applications and thus, address the needs of the industry.

1.4 Objectives

1.4.1 General Objective

The main objective of this thesis work is to study and analyze the performance of non-blind adaptive equalizers that can be used in broadcast channels.

1.4.2 Specific Objectives

The specific objectives of this thesis work are:

- To understand the effect of multipath propagation on signal reception in broadcasting channels.
- To study the non-blind adaptive equalization techniques that can be used to mitigate the problem of ISI in broadcast channels.
- To review selected non-blind equalization techniques; namely, ZF, MMSE, LMS, RLS, DFE and MLSE techniques and compare their performance in terms of their BER minimization, rate of convergence, stability and computational complexity to propose one appropriate technique for simulation.
- To implement the proposed equalizer in MATLAB software for functionality test in broadcast channels and investigate its performance.

1.5 Contributions of the Thesis

The main contribution of this thesis work is to study and compare the performances of ZF, MMSE, LMS, RLS, DFE and MLSE algorithm based equalizers so that the best performing equalizer can be proposed for implementation for local broadcast channel applications. Since the thesis work is initiated as a result of interests form a sponsor industry to implement efficient digital receivers, the results of this work can be used as an input to the intended industry. It will help them through their way in achieving their goal of implementing fast and reliable wireless digital communication system.

1.6 Methodology

The methods employed to achieve the objective of this thesis work are:

- **Literature review**: this includes the survey and reading of books, articles, journals, white papers, simulation tools and all forms of other resources which are related to channel equalization techniques.
- **System modeling**: this involves modeling of the overall end-to-end communication link including, the input generation, input processing, encoding, modulation and pulse shaping in the transmitter part as well as their counterparts in the receiver together with the channel modeling and equalization technique employed at the receiver.
- **Simulation**: this is the approximation of the modeled communication system in MATLAB software, such that performance investigation and functionality tests can be carried out with randomly generated data or stored image signal.
- **Performance comparison**: this involves the convergence speed, stability, complexity and BER performance comparisons of the selected equalization techniques.
- **Analysis and interpretation of the results**: this is the performance analysis and interpretation of the implementation which is based on the results and findings obtained from the simulated system.

1.8 Scope and Limitations of the Thesis

The scope of this thesis work is limited to performance analysis of non-blind channel equalizers specifically ZF, MMSE LMS, RLS, DFE and MLSE equalizers that can be used to mitigate the frequency selectivity effect of broadcast channels and implementation of the appropriate equalizer for simulation in MATLAB. Then, based on the performance analysis, the best performing equalizer will be selected for practical implementation. However, the implementation will be only in MATLAB software and it will not include hardware implementation. For simulation, a random integer input generated using MATLAB's built-in function will be used for the BER comparison whereas stored image source signal will be used to test the practical implementation. The thesis work will not include the implementation and analysis of blind and semi-blind types of equalization techniques as they are not the focus of the work due to their complex computational load when compared to the non-blind equalizers.

1.8 Literature Review

Channel equalizers are well known systems in wireless digital communication system applications since the early 1960's and many researches and literatures have been published across different parts of the world on this issue for several years. It is usually the topic of a separate chapter in leading books on wireless and digital communication systems (like Proakis 2000; David Tse 2004; Goldsmith 2005; Miao 2007; Wesolowski 2009; Molisch 2011) and separate books also tackle this subject as well (Clark 1985; Ding and Ye 2001; Gregory Bottomley 2011). Adaptive equalization algorithms are also a well-documented application examples in books devoted to adaptive filters (Macchi 1995; Haykin 2002).

Especially in the last decades following the emergence of information demanding systems, many scholars and researchers in different times have developed too many algorithms that can be used for equalizer designs in different scenarios. From those many literatures published on the issue of channel equalization, the following four papers are selected to be discussed in this section.

The first one goes to the works of **Samuel Jalali** that discussed and simulated many equalization techniques including the blind and training based equalizers in different channel models for neural network application. The paper presents the application of a new and modified neural networks requiring very short training period for the proper channel equalization in supervised mode. For blind modes, the concept of multiple cooperative algorithms were discussed for the cases of two and three cooperative algorithms. The paper also used the "select absolutely larger equalized signal" and "majority vote" methods for 2 and 3-algorithm systems respectively [6].

Authors in [9] also presented the performance analysis of LMS, RLS and CMA equalization algorithms in the case of noisy audio signal. According to their work, the RLS equalizer has better convergence rate than the LMS and CMA equalizers whose convergence rate is highly dependent on the selection of the step size. They also conclude that in the presence of noisy audio source, the CMA equalizer provides better performance than the LMS and comparable to the RLS algorithm and requires no much computing power.

Saptrashi Das used Basis Expansion Method (BEM) and Complex Exponential Basis Expansion Model (CE-BEM) for estimating and equalizing high mobility doubly selective channels [9]. The paper implements a Rayleigh Fading channel with Jakes Doppler spectrum which is the simplified form of Clerk's model. The implementation was done in this work for Worldwide Interoperability for Microwave Access (WiMAX) and recommends the implementation of equalizers that use BEM coefficients directly, without ever creating the channel matrix in other applications like digital DVB-T systems and wireless access in vehicular environment (WAVE) [10].

Lorena Martinez Jimenez described the application of BEM for doubly selective channel equalizers and used together with semi-blind type equalization technique namely, coded decision directed demodulation (CD3) algorithm. The paper discusses the implementation and simulation of proposed equalization techniques in TU6 and RA6 models. The paper also suggests the implementation of modified BEM (CE-BEM) and modified CD3 schemes. The proposed schemes were named proposed scheme 1 which substitutes the ideal one-tap frequency domain equalizer by the belief propagation detector and maintains the time interleaver, whereas the second proposed scheme 2 removes the time interleaver and incorporates the turbo principle instead [1].

1.9 Thesis Organization

This thesis consists of six main chapters. The first one is an introductory part which mainly includes the background, goal and motivational aspects of the thesis. The second Chapter presents the fading channel characteristics and modeling of the broadcast channels considered for this piece of work. Whereas, the third Chapter deals with the generic presentation of equalization techniques including their classification as well as further mathematical description and implementation details of selected equalization schemes. The fourth Chapter deals with the end to end system model of communication system and tries to describe each block used in the model. The fifth Chapter includes simulation of the modeled communication system as well as analysis and interpretation of the outcomes. The last Chapter is the conclusion and recommendation part of the thesis which tries to discuss the important conclusions drawn based on the results obtained from the whole thesis work.

Chapter Two

Channel Fading and Broadcast Channel Characterization

2.1 Introduction

Physical channels used in transmission of digital signals can be rarely represented by a non-distorting channel model with AWGN as the only impairment. The only channel that can be represented by a band-limited AWGN channel model is a microwave line of sight (LOS) channel. The rest channel types used in wireless system applications are characterized not only by a limited bandwidth but also by a channel transfer function in which particular frequency components of transmitted signals are unequally attenuated (causing amplitude distortion) and unequally delayed (creating delay distortion). These effects are the result of the physical properties of the transmission medium and the imperfect design of transmitter and receiver filters applied in the transmission system [3]. This chapter describes some important characteristics and physical properties of a transmission medium including the characterization of multipath fading channel and the broadcast channel to be employed for this particular thesis work.

2.2 Multipath Fading Channel

The presence of multiple scatterers as shown in Figure 2.1 below (like buildings, trees, mountains, vehicles, hills, and so on) causes a transmitted signal to propagate along several different paths that terminate at the receiver. As a result, the receiver antenna captures a superposition of multiple attenuated copies of the transmitted signal. This phenomenon is referred to as multipath propagation. Due to different lengths of the propagation paths, the individual multipath components experience different delays (time shifts). These multipath signals with different attenuation levels and random phases combine at the receiver to give a resultant signal with random fluctuations and these random fluctuations in the received signal are called *fading* [2].

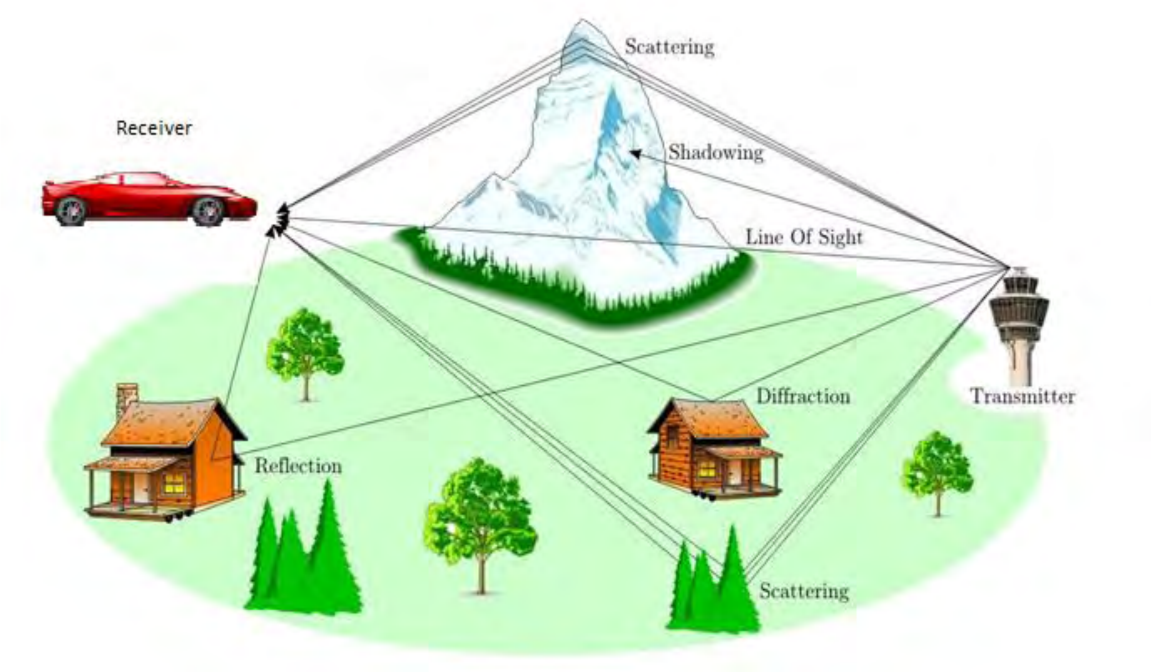

Figure 2.1: Multipath propagation [11]

Thus if a single pulse is transmitted over a multipath channel then the received signal will appear as a pulse train, with each pulse in the train corresponding to the LOS component or a distinct multipath component associated with a distinct scatterer or cluster of scatterers. The time delay spread of a multipath channel can result in significant distortion of the received signal. This delay spread equals the time delay between the arrivals of the first and last received signal components associated with a single transmitted pulse. If the delay spread is small compared to the inverse of the signal bandwidth, then there is little time spreading in the received signal. However, if the delay spread is relatively large then there is significant time spreading of the received signal, which can lead to substantial signal distortion [4], [12].

Another characteristic of the multipath channel is its time-varying nature. This time variation arises when either the transmitter or the receiver is moving and hence the location of reflectors in the transmission path, which gives rise to multipath, will change over time. Thus, if pulses repeatedly transmitted from a moving transmitter, changes will be observed in the amplitudes, delays, and number of multipath components corresponding to each pulse. However, these changes occur over a much larger time scale than the fading due to constructive and destructive addition of multipath components associated with a fixed set of scatterers [4].

In addition to the multipath effects also known as small-scale fading, there is also another type of fading known as shadowing or large scale fading. It is caused by high rise buildings and hills standing between the transmitter and receiver, where the receiver is shadowed by these obstacles. Shadowing results in attenuation of the received signal power.

In most environments, the path loss is sufficiently variable that it must be characterized statistically. This is particularly true for mobile communications where either or both terminals may be moving (changing the relative geometry) and where both are using wide-angle or omnidirectional antennas. Multipath models vary depending on the type of environment and the frequencies involved. While detailed databases of most urban areas are available, statistical modeling based on empirical data (often fitted to specific empirical data) is still the method of choice [6]. The next sections present the large and small scale fading characteristics.

2.2.1 Large Scale Fading

In general, the average power of the received signal decreases logarithmically with the distance between the transmitter and the receiver. The attenuation caused by the distance is called large scale fading or path loss. The propagation medium and the environment would also have some effect on the total loss of the signal strength. The averaged received power at a certain distance from the transmitter is measured by keeping the distance to the transmitter constant (as the radius of a circle) and moving the receiver antenna on the circle. The difference between the transmitted power p_t and the averaged received signal power $p(d)$ (expressed in dBm) at certain distance is the path loss in dB, which is denoted by $L(d)$ [13].

$$p(d) = p_t - L(d), \qquad d > d_0 \tag{2.1}$$

The average of the path loss in dB units, with respect to a referenced distance d_0 at which the path loss is measured and is known, is given by [13]:

$$\bar{L}(d) = \bar{L}(d_0) + 10n\log_{10}(\frac{d}{d_0}) \tag{2.2}$$

The order n has the constant value of 2 for LOS links but is usually higher than 2 for multipath channels in cities and urban areas. The model in Eq. (2.2) is known as the log-distance path loss model. The measured path loss $L(d)$ at distance d can be significantly different from the average value due to, for example, shadowing effects, and in fact, is a Gaussian random variable given by [13]:

$$L(d) = \bar{L}(d_0) + 10n\log_{10}(\frac{d}{d_0}) + X_\sigma \tag{2.3}$$

where, X_σ is a zero-mean Gaussian random variable (in dB) with standard deviation σ also expressed (in dB). The path loss described is known as log-normal shadowing.

The various measurements of path loss at different distances are collected in a graph of loss in dB versus the distance also (in dB). The constant n can be approximated by the best fitting line of the data [13].

2.2.2 Small Scale Fading

For most practical channels, large scale propagation model is inadequate to describe the channel and predict system performance. Small-scale fading is used to describe the rapid fluctuations of the amplitude and phases of a radio signal over a short period of time, so that large-scale path loss effects could be ignored [13].

There are a variety of ways to statistically model the wireless channels in order to represent the random behavior of multipath fading. One simple and popular model represents the fading channel with a linear and time-varying channel impulse response denoted by the function $h(t, \tau)$ in Figure 2.2 below [6].

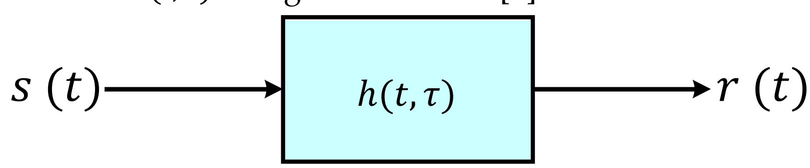

Figure 2.2: Channel modeling by channel impulse response [6]

This channel representation can be characterized by stochastic channel models which will be discussed in Section 2.3 of this paper. But here, important time and frequency dispersion parameters that can be used to characterize communication channels are discussed.

2.2.2.1 Time Dispersion parameters

A perfect channel from a communications point of view is one that has a constant gain and a linear phase response, or at least possesses these features over a desired frequency range. Such a frequency range should be larger than the frequency spectrum of the transmitted signal to preserve the signal spectral characteristics. Consequently, such an ideal channel can be symbolically shown as $h(t, \tau) = g_0 \delta(\tau)$, with g_0 constant [6].

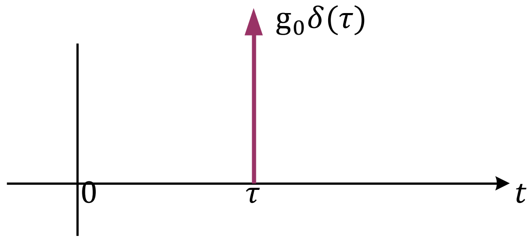

Figure 2.3: Ideal channel impulse response [6]

Such channel impulse response implies only one received signal delayed by τ, causing no ISI even when the gain varies with time as the varying response of $h(t,\tau) = g_0\delta(\tau)$, where $g(t)$ is relatively slowly varying function of time and in general may be complex valued. If it is assumed that the multipath channel includes N different paths, and if the attenuation of k^{th} multipath component is denoted by α_k, the delay of k^{th} multipath component by τ_k and the power of k^{th} component by $P(\tau_k)$, then the weighted average delay (also known as mean excess delay) can be defined as [13]:

$$\bar{\tau} = \frac{\sum_{k=1}^{N} \alpha^2{}_k \tau_k}{\sum_{k=1}^{N} \alpha^2{}_k} = \frac{\sum_{k=1}^{N} P(\tau_k)\tau_k}{\sum_{k=1}^{N} P(\tau_k)} \tag{2.4}$$

The second statistical moment of the delay spread may also be computed by [13]:

$$\overline{\tau^2} = \frac{\sum_{k=1}^{N} \alpha^2{}_k \tau^2{}_k}{\sum_{k=1}^{N} \alpha^2{}_k} = \frac{\sum_{k=1}^{N} P(\tau_k)\tau^2{}_k}{\sum_{k=1}^{N} P(\tau_k)} \tag{2.5}$$

The channel delay spread, that is the RMS value of the delay, is given by [13]:

$$\sigma_\tau = \sqrt{\overline{\tau^2} - (\bar{\tau})^2} \tag{2.6}$$

The channels with time-dependent response given by $h(t,\tau)$ will have time-dependent frequency response $H(\omega, t)$ with [6];

$$H(\omega, t) = \int_{-\infty}^{\infty} \mathrm{h}(\mathrm{t}, \tau)\, \mathrm{e}^{-j\omega\tau} d\tau \tag{2.7}$$

To determine the wireless channel characteristics in the frequency domain, the correlation coefficient or factor of the channel frequency response has to be determined first based on a change in frequency of the size $\Delta\omega$ [13].

$$P(\Delta\omega) = \frac{E\{H^*(\omega, t)H(\omega + \Delta\omega, t)\}}{E\{H^*(\omega, t)H(\omega, t)\}} = \frac{\int_{-\infty}^{\infty} |\mathrm{h}(\mathrm{t}, \tau)|^2\, \mathrm{e}^{-j\Delta\omega\tau} d\tau}{\int_{-\infty}^{\infty} |\mathrm{h}(\mathrm{t}, \tau)|^2 d\tau} \tag{2.8}$$

The coherence bandwidth is the counterpart of the delay spread in the frequency domain, and it is the range of frequencies over which the channel gain remains about the same, or as is commonly known, over the range of frequencies the gain is flat, with a linear phase. Fortunately, the coherence bandwidth of the channel denoted by B_c can be approximated based on the specified correlation coefficient value.

The case when the correlation coefficient is about zero, $P(\Delta\omega) \approx 0, \Delta\omega = 2\pi B_c$. The coherence bandwidth for this case is approximated by $B_c = \frac{1}{\sigma_\tau}$, which implies that changing the frequency by B_c results in a completely different (and statistically independent) gain [13].

For the more common value of $P(\Delta\omega) \approx 0.5$, the coherence bandwidth is estimated by, $B_c = \frac{1}{5\sigma_\tau}$ which implies that the channel gain at ω and $\omega + B_c$ are similar. Finally, considering $P(\Delta\omega) \approx 0.9$, the coherence bandwidth can be approximated as $B_c = \frac{1}{5\sigma_\tau}$. In this case, the channel gain at ω is almost exactly the same as the gain at $\omega + B_c$ [13].

2.2.2.2 Frequency Dispersion Parameters

The mobility of the communicator originates another parameter known as Doppler shift in frequency, or simply some change in frequency due to the mobile velocity.

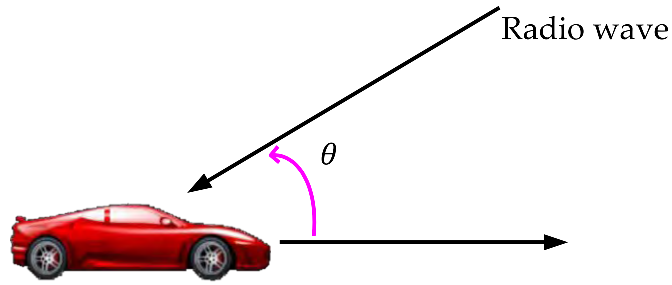

Figure 2.4: Doppler shift geometry [6]

It is denoted by f_d and computed as $f_d = \frac{v}{\lambda}\cos\theta$, where v is the relative receiver speed, λ the radio wavelength, and θ is the angle between the wave direction and the mobile direction. The change in frequency is positive when the receiver approaches the transmitter and negative when it is departing [13], [14].

It is obvious that different paths have different Doppler shifts that possess random natures, as the angle θ can be considered random and in most cases uniformly distributed. As a result, there can be a number of copies of the transmitted waves at the receiver antenna, each travelling along different paths, which are characterized by various relative speeds and angles. Moreover, in specific scenarios, the surrounding objects might be moving and generating time varying Doppler shifts on multiple components. The corresponding random change in frequency causes spectral broadening known as *Doppler spread* [15], [16]. It is defined as the range of frequencies over which the Doppler shift is not zero and denote by B_d in this paper.

The time domain properties of wireless channels can be further specified by defining another parameter, coherence time, which is the duration of time in which the channel impulse response is invariant. Two samples of the channel are highly correlated if their time separation is less than the coherence time. The given definition itself depends on the time correlation coefficient [17], [18].

The correlation coefficient in the time domain as a function of time difference Δt is given by [13]:

$$p(\Delta t) = \frac{E\{h(t)h^{*}(t+\Delta t)\}}{E\{|h(t)|^{2}\}} \tag{2.9}$$

Generally, the coherence time is inversely proportional to the Doppler spread [13].

$$T_c = \frac{1}{B_d} \tag{2.10}$$

If the coherence time for which the time correlation coefficient of Eq. (2.9) remains above 0.5, it is approximated by [13]:

$$T_c = \frac{9}{16\pi B_d} \tag{2.11}$$

As a rule of thumb, the geometric average of Eq. (2.10) and Eq. (2.11) is used for digital communication and it can be given as [13]:

$$T_c = \sqrt{\frac{1}{B_d} . \frac{9}{16\pi B_d}} \approx \frac{0.423}{B_d} \tag{2.12}$$

2.2.3 Small Scale Fading Types

Depending on the relationship between the signal parameters (such as bandwidth and symbol period) and the channel parameters (such as delay spread and Doppler spread), different transmitted signals will undergo different types of fading. The time-dispersion which is a result of multiple delay spread and frequency dispersion which is a result of Doppler spread result in four distinct propagation effects. Hence, small scale fading can be categorized as flat fading or frequency selective fading and slow fading or fast fading based on time delay spreading of the signal and time variant nature of the channel respectively [13].

2.2.3.1 Fading Effects Due to Multipath Time Delay Spread

Time dispersion due to multipath causes the transmitted signal to undergo either flat or frequency-selective fading.

2.2.3.1.1 Flat Fading Channel

The coherence bandwidth of the channel, B_c, is greater than the bandwidth of the transmitted signal, $B_s = 1/Ts$, where Ts is the symbol duration such that all frequency components of the signal will experience the same magnitude of fading. The coherence bandwidth, B_c is a statistical measure of the range of frequencies over which the channel passes all spectral components with approximately equal gain and linear phase.

Flat fading could also be viewed in time domain, to be the result of a multipath propagation whose delay spread, σ_τ, is so small compared to the symbol duration, Ts , that they add up to one undistorted signal (or the received signal is not distorted by ISI). To summarize, a signal undergoes flat fading if $T_s \gg \sigma_\tau$ and $B_s \ll B_c$ [13], [19].

2.2.3.1.2 Frequency Selective Channel

In this case the coherence bandwidth of the channel is smaller than the bandwidth of the signal such that different frequency components of the signal will be affected differently by the channel. In the time domain, the multipath components of the signal will have significant time dispersion compared to the symbol period and this result in ISI. To summarize, a signal undergoes frequency-selective fading if $T_s < \sigma_\tau$ and $B_s > B_c$ [13], [19].

2.2.3.2 Fading Effects Due to Doppler Spread

Depending on how rapidly the transmitted signal changes as compared to the rate of change of the channel, a channel may be classified as slow fading or fast fading channel.

2.2.3.2.1 Slow Fading Channel

It occurs when the coherence time of the channel is greater than the symbol duration of the transmitted signal. In frequency domain the Doppler spread of the channel is much less than the transmitted signal. In this channel, the amplitude and phase change imposed by the channel can be considered roughly constant over the period of channel use. To summarize, a signal undergoes frequency-selective fading if $T_s \ll T_c$ and $B_s \gg B_d$ [13], [19].

2.2.3.2.2 Fast Fading Channel

In this case the channel impulse response changes rapidly within the symbol duration. This is when the coherence time of the channel is small relative to the symbol duration of the transmitted signal. In frequency domain, signal distortion due to fast fading increases with increasing Doppler spread relative to the bandwidth of the transmitted signal. In this case, the amplitude and phase change imposed by the channel varies considerably over the period of channel use. To summarize, a signal undergoes frequency-selective fading if $T_s > T_c$ and $B_s < B_d$ [13], [19].

2.3 Broadcast Channel Characteristics

Bello's Wide Sense Stationary Uncorrelated Scattering (WSSUS) model has been accepted widely as an appropriate stochastic model for time-variant frequency-selective wireless channels. This model, which is valid for most radio channels, assumes that the channel is stationary in the wide sense and that the scattered components with different propagation delays are statistically uncorrelated. The broadcast channel considered in this work is also represented by this model and the description of frequency-selective stochastic channel models, specifically the well-known WSSUS channel model is presented below. In particular, stochastic system functions as well as the characteristic quantities derivable from these functions will be introduced to characterize the statistical properties of WSSUS channel models. These models are especially well suited for the modeling of the radio channels specified by the European working group Cooperation in Science and Technology (COST 207) [20], [21], [22].

2.3.1 Frequency-Selective Stochastic Channel Models

2.3.1.1 WSSUS Model According to Bello

The WSSUS model enables the statistical description of the input-output relationship of radio channels for the transmission of band-pass signals in the equivalent complex baseband for observation periods in which the stationarity of the channel is ensured in the wide sense [20], [22]. It is a combination of Wide Sense Stationary (WSS) and Uncorrelated Scattering (US) models [20].

2.3.1.1.1 WSS Model

In this channel model, the impulse response of the channel is considered WSS which means the channel impulse response is independent of time t. In other words, the autocorrelation function $R_{hh}(t,\tau)$ is independent of time instant t and it depends on the difference between the time instants $\Delta t = t_2 - t_1$ where $t_1 = t$ and $t_2 = t + \Delta t$. The autocorrelation function for WSS channel model is expressed as [20], [22]

$$R_{hh}(\Delta t; \tau_1, \tau_2) = E[h(t,\tau_1)h*(t+\Delta t, \tau_2) \qquad (2.13)$$

2.3.1.1.2 US Model

A second important class of channel models is obtained by assuming that scattering components with different propagation delays are statistically uncorrelated. These channel models are called US channel models. Here, the individual scattered components arriving at the receiver front end (at different propagation delays) are assumed to be uncorrelated. Thus the autocorrelation function can be expressed as [20]

$$R_{hh}(t_1, t_2; \tau_1, \tau_2) = R_{hh}(t_1, t_2; \tau_1)\delta(\tau_1 - \tau_2) \qquad (2.14)$$

2.3.1.1.3 WSSUS Models

The WSSUS channel model combines the aspects of WSS and US channel model that are discussed above. Here, the channel is considered as stationary in wide sense and the scattering components arriving at the receiver are assumed to be uncorrelated. Combining both the properties, the autocorrelation function $R_{hh}(\Delta t, \tau)$ becomes [20], [22]

$$R_{hh}(\Delta t, \tau) = E[h(t, \tau)h*(t + \Delta t, \tau)] \tag{2.15}$$

2.3.1.2 Scattering Function

The autocorrelation function of the WSSUS channel model can be represented in frequency domain by taking Fourier transform with respect one or both variables- difference in time Δt and the propagation delay τ. Of the two forms, the Fourier transform on the variable Δt gives specific insight to channel properties in terms of propagation delay and the Doppler Frequency simultaneously. The Fourier transform of the above two-dimensional autocorrelation function on the variable Δt is called *scattering function* and is given by [20], [22];

$$S(f, \tau) = \int_{-\infty}^{\infty} R_{hh}(\Delta t, \tau) e^{-j2\pi f_d \Delta t} d\Delta t \tag{2.16}$$

Thus, the scattering function is a function of two variables: *Doppler Frequency* f_d and the *propagation delay* τ. It gives the average output power of the channel as a function of Doppler Frequency f_d and the propagation delay τ [20].

Two important relationships can be derived from the scattering function. These relationships are power delay profile and Doppler power spectrum**.** Both of them affect the performance of a given wireless channel. Power delay profile is a function of propagation delay and the Doppler power spectrum is a function of Doppler Frequency.

Power delay profile $S_\tau(\tau)$ gives the signal intensity received over a multipath channel as a function of propagation delays. It is obtained as the spatial average of the complex baseband channel impulse response as [20], [22]

$$S_\tau(\tau) = R_{hh}(0,\tau) = E[|h(t,\tau)|^2] \tag{2.17}$$

Power delay profile can also be obtained from scattering function, by integrating it over the entire frequency range (removing the dependence on Doppler frequency) [20], [22].

$$S_\tau(\tau) = \int_{-\infty}^{\infty} S(f,\tau)df \tag{2.18}$$

Similarly, the Doppler power spectrum can be obtained by integrating the scattering function over the entire range of propagation delays [20], [22].

$$S_{\mu\mu}(f) = \int_{-\infty}^{\infty} S(f,\tau)d\tau \tag{2.19}$$

2.3.1.3 The COST 207 Channel Models

Based on the WSSUS assumption, the working group COST 207 developed specifications for the delay and Doppler power spectral densities of four different propagation environments. These propagation environments were classified into areas with rural area (RA) character, TU for areas which are typical for cities and suburbs, bad urban (BU) for densely built urban areas with bad propagation conditions, and hilly terrains (HT). The delay power spectral density functions specified for those propagation environments are given below [20], [22].

RA propagation environments:

The power delay spectral density for RA environments is given as [20], [22];

$$S_\tau(\tau) = \begin{cases} C_{RA}e^{-9.2\tau/\mu s}, & 0 \le \tau < 0.7\mu s \\ 0, & else \end{cases} \tag{2.20}$$

where, C_{RA} is a real valued constant coefficient given by:

$$C_{RA} = \frac{9.2}{1 - e^{-6.44}} \tag{2.21}$$

The delay spread $\sigma_\tau = 0.1\mu s$ for this case.

TU propagation environments:

Whereas, the power delay spectral density for TU environments is given as [20], [22];

$$S_\tau(\tau) = \begin{cases} C_{TU} e^{-\tau/\mu s}, & 0 \le \tau < 7\mu s \\ 0, & else \end{cases} \tag{2.22}$$

where, C_{TU} is a real valued constant coefficient given by:

$$C_{TU} = \frac{1}{1 - e^{-7}} \tag{2.23}$$

The delay spread $\sigma_\tau = 1.1\mu s$ for TU propagation and it will be the focus of this thesis work.

BU propagation environments:

And, the power delay spectral density for TU environments is given as [20], [22];

$$S_\tau(\tau) = \begin{cases} C_{BU} e^{-\tau/\mu s}, & 0 \le \tau < 5\mu s \\ C_{BU} \frac{1}{2} e^{(5-\tau/\mu s)}, & 5\mu s \le \tau < 10\mu s \\ 0, & else \end{cases} \tag{2.24}$$

where, C_{BU} is a real valued constant coefficient given by:

$$C_{BU} = \frac{2}{3(1 - e^{-5})} \tag{2.25}$$

The delay spread $\sigma_\tau = 2.53\mu s$ for BU propagation.

HT propagation environments:

Finally, the power delay spectral density for HT environments is given as [20], [22];

$$S_\tau(\tau) = \begin{cases} C_{HT} e^{-3.5\tau/\mu s}, & 0 \le \tau < 2\mu s \\ C_{HT} 0.1 e^{(15-\tau/\mu s)}, & 15\mu s \le \tau < 10\mu s \\ 0, & else \end{cases} \tag{2.26}$$

where, C_{HT} is a real valued constant coefficient given by:

$$C_{HT} = \frac{2}{3(1 - e^{-5})} \tag{2.27}$$

The delay spread $\sigma_\tau = 6.88\mu s$ for HT propagation. Figure 2.5 below depicts the power delay profile of each of the above propagation environments.

The COST 207 models also specified four different Doppler spectra. These are; Jakes, GAUSE I, GAUSE II and RICE spectra [20], [22].

Jakes: The classical Jakes spectrum occurs only in the case of path delays less than 500ns, i.e., $\tau < 0.5\mu s$, and given by [20], [22];

$$S_{\mu\mu}(f) = \frac{1}{\pi f_d \sqrt{1 - (\frac{f}{f_d})^2}}, \quad |f| \le f_d \tag{2.28}$$

where f_d represents the maximum Doppler frequency and the Doppler spread is $B_d = \frac{f_d}{\sqrt{2}}$.

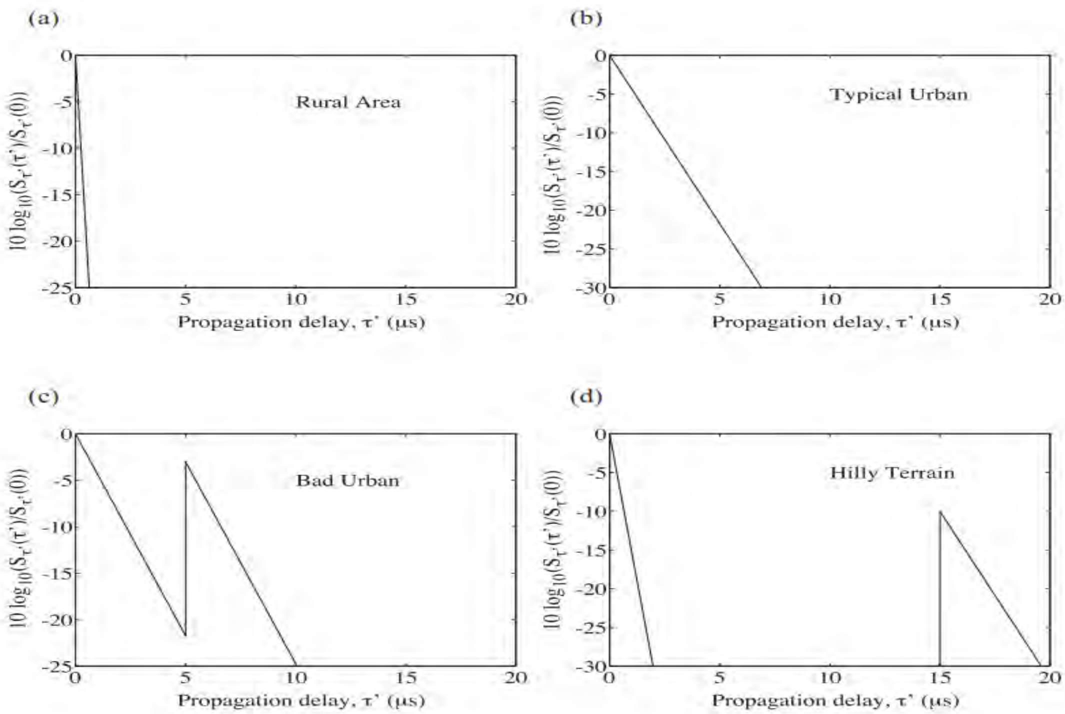

Figure 2.5: Delay power spectral densities of channel models according to COST 207 [20], [22]

GAUS I: GAUS I is the sum of two Gaussian functions, occurs only in the case of path delays in the range of $500ns$ to $2\mu s$, i.e., $0.5\mu s \leq \tau < 2\mu s$ and is given by [20], [22];

$$S_{\mu\mu}(f) = G(A_1, -0.8f_d, 0.05f_d) + G\left({}^{A_1}/_{10}, 0.4f_d, 0.1f_d\right) \tag{2.29}$$

where $G(A_i, f_i, s_i)$ is defined as $G(A_1, f_1, s_1) = A_1 e^{\frac{-(f-f_1)^2}{2{s_1}^2}}$, the value of A_1 is given by $A_1 = \frac{50}{\sqrt{2\pi}3f_d}$, f_1 & $s_1$are the values of the second and third terms of the Gaussian functions in Eq. (2.29) respectively. The Doppler spread for this case is given by $B_d = 0.45f_d$.

GAUSE II: GAUSE II is the sum of two Gaussian functions, occurs only in the case of path delays greater than $2\mu s$, i.e., $\tau \geq 2\mu s$ and is given by [20], [22];

$$S_{\mu\mu}(f) = G(A_2, 0.7f_d, 0.1f_d) + G\left({}^{A_2}/_{10^{1.5}}, 0.4f_d, 0.15f_d\right) \tag{2.30}$$

where $G(A_2, f_2, s_2)$ is given by $G(A_2, f_2, s_2) = A_2 e^{\frac{-(f-f_2)^2}{2s_2^2}}$ and the value of A_2 is given by $A_2 = \frac{10^{1.5}}{\sqrt{2\pi}[\sqrt{10}+0.15)f_d]}$. Ones again, f_2 & s_2 are the values of the second and third terms of the Gaussian functions in Eq. (2.30) respectively.

The Doppler spread for GAUSE II spectrum is $0.25f_d$

RICE: RICE Doppler spectrum is obtained by combining the Jakes Doppler spectrum with and LOS component path. It is given by [20], [22];

$$S_{\mu\mu}(f) = \frac{1}{\pi f_d \sqrt{1-(\frac{f}{f_d})^2}} + 0.91\delta(f - 0.7f_d), \quad |f| \leq f_d \tag{2.31}$$

The Doppler spread is $0.39f_d$ for this case.

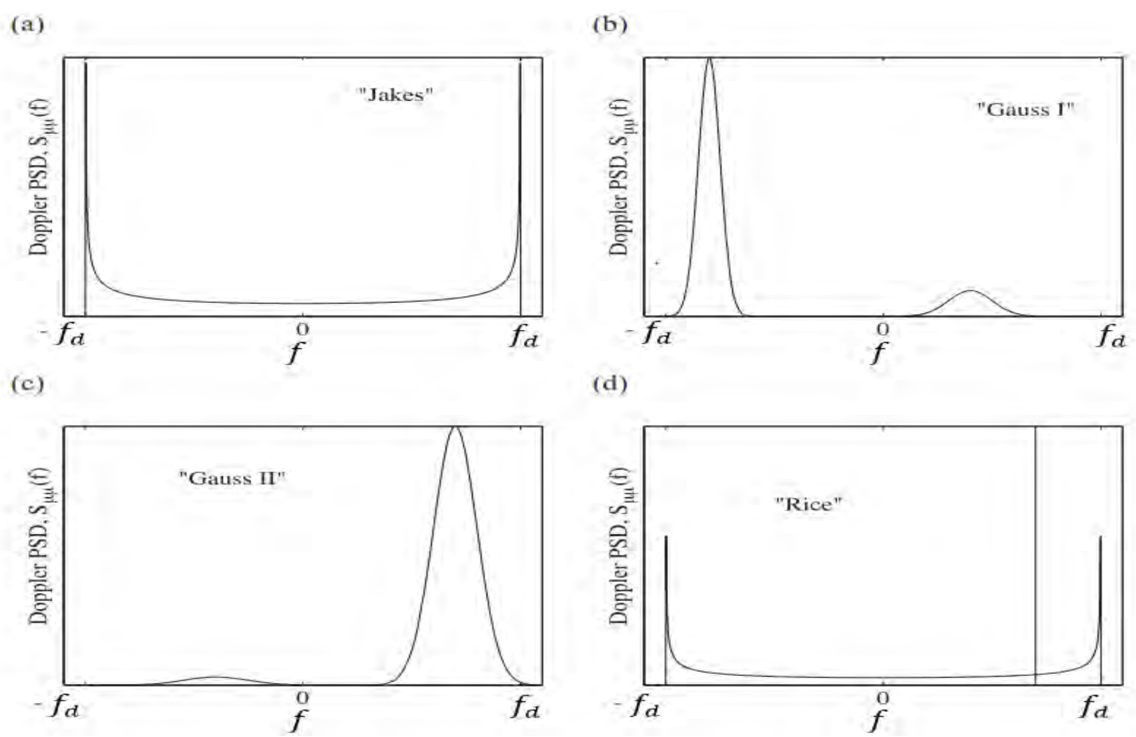

Figure 2.6: Doppler power spectral densities of channel models according to COST 207 [20], [22]

Chapter Three

Channel Equalization Techniques

3.1 Introduction to Channel Equalization

In a broad sense, equalization defines any signal processing technique used at the receiver to alleviate the ISI problem caused by delay spread. Especially higher data-rate applications are more sensitive to delay spread and require high-performance equalizers at the receiver or other ISI mitigation techniques to be used at the transmitter side (like spread-spectrum and multicarrier modulation) to make the signal less susceptible to delay spread. In this chapter various issues associated with equalizer design starting from their mathematical framework to the various points regarding to some equalization techniques selected for this thesis work are discussed.

3.1.1 Mathematical Framework of Channel Equalizers

Figure 3.1 below illustrates the communication model with channel equalizer. The signal received by the equalizer is given by

$$x(t) = d(t) * f(t) + n(t) \tag{3.1}$$

where $d(t)$ is the transmitted signal, $n(t)$ denotes the baseband noise and $f(t)$ is the combined impulse response of the transmitter, channel and receiver filters.

If the impulse response of the equalizer is $h_{eq}(t)$, the output of the equalizer will be;

$$\hat{y}(t) = d(t) * f(t) * h_{eq}(t) + n(t) * h_{eq}(t) = d(t) * g(t) + n(t) * h_{eq}(t) \tag{3.2}$$

However, the desired output of the equalizer is $d(t)$ which is the original source data. Assuming $n(t) = 0$, it is required to force $\hat{y}(t)$ to be equivalent with $d(t)$, and to do that $g(t)$ must be equal to:

$$g(t) = f(t) * h_{eq}(t) = \delta(t) \tag{3.3}$$

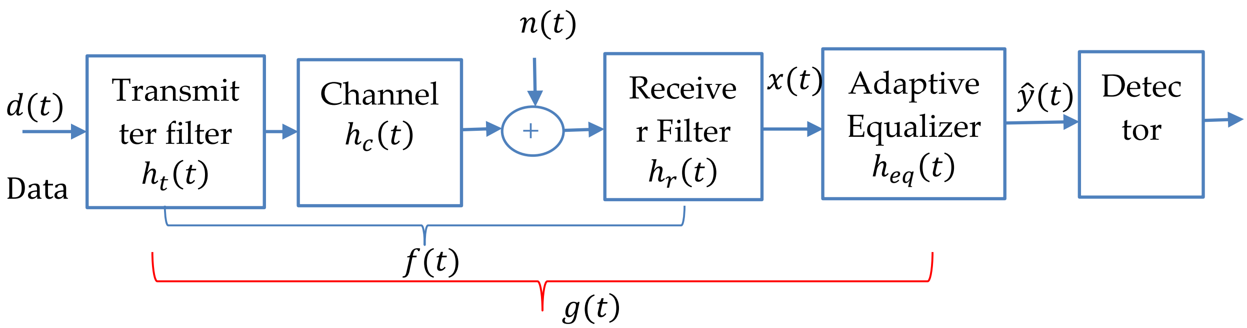

Figure 3.1: Communication system model with equalizer [12]

In frequency domain it can be written as;

$$G(f) = F(f).H_{eq}(f) = 1 \tag{3.4}$$

The frequency response of the equalizer should be designed to satisfy the following equation:

$$H_{eq}(f) = \frac{1}{F(f)} \tag{3.5}$$

Hence, the main goal of any equalizer is to satisfy Eq. (3.5) optimally, which indicates that an equalizer is ideally an inverse filter of the channel. However, this equalizer design must typically balance ISI mitigation with noise enhancement, since both the signal and the noise pass through the equalizer, which can increase the noise power.

3.2 Classification of Equalization Techniques

Channel equalizers can be classified in several different ways. One criterion of the classifications is whether they are adaptive equalizers or non-adaptive equalizers. Adaptive equalizers are used when the channel is time varying by changing their filter coefficients according to the time-varying channel. Non-adaptive equalizers are used for time invariant channels and designed by the inverse function of the channel response [12], [23].

Equalization techniques can also be classified in to three major categories namely non-blind, blind and semi-blind equalizers. The first one is non-blind equalization which requires an initial training period, during which a known data sequence is transmitted together with the message signal. A replica of this sequence is made available at the receiver in proper synchronism with the transmitter, thereby making it possible for adjustments to be made to the equalizer coefficients in accordance with the adaptive filtering algorithm employed in equalizer design. When training signals are entirely absent, the transmission is called blind, and adaptive algorithms for estimating the transferred symbols and possibly estimating the channel are called blind algorithms. Since, training information is not available; a reliable reference is missing, leading to a very slow learning behavior in such algorithms. Thus, blind methods are typically of interest when a large amount of data is available and quick detection is not important. The third one is semi-blind equalization in which blind methods are used together with training symbols in order to improve the drawbacks of both blind and non-blind methods.

Another criterion of the classifications is whether they are linear or non- linear equalizers. The linear equalizers are based on the tap delayed equalization. They do not have a feedback path. The output is linear combination of the inputs. On the other hand, the non-linear equalizers have a feedback path and are used when a receiver copes with a large ISI and deep fading [12].

Equalizers can also be categorized as symbol-by-symbol (SBS) or sequence estimators (SEs). SBS equalizers remove ISI from each symbol and then detect each symbol individually. All linear equalizers in Figure 3.2 (as well as the DFE) are SBS equalizers. SEs detect sequences of symbols, so the effect of ISI is part of the estimation process. MLSE equalizer is the optimal form of SE [12].

In addition to the equalizer type and structure, adaptive equalizers require algorithms for updating the filter tap coefficients during training and tracking. Many algorithms have been developed over the years for this purpose, and they generally incorporate trade-offs between complexity, convergence rate, and numerical stability. Figure 3.2 below summarizes the different equalizer types along with their corresponding structures and tap updating algorithms [2], [12].

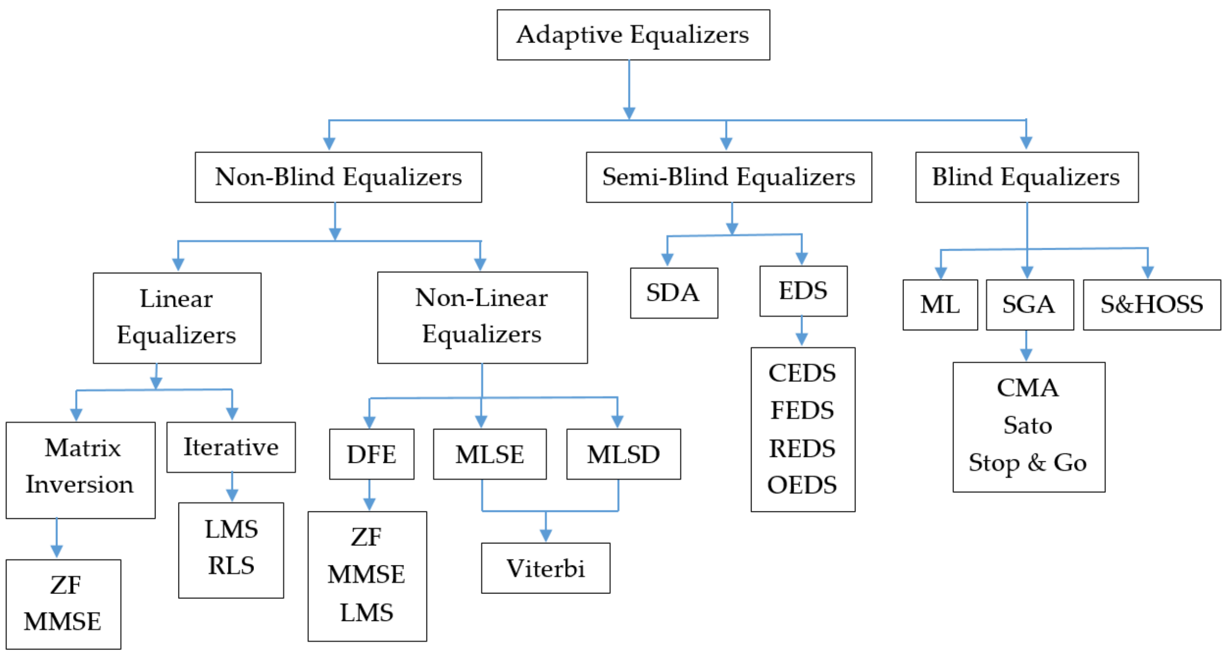

Figure 3.2: Classifications of equalization techniques [12], [13]

3.3 Training Based Equalization Techniques

Most of the equalization techniques work in non-blind mode in which the receiver is supervised by a copy of the transmitted signal. It consists of two stages which are training and detection phases. During the training phase, a known bit sequence is transmitted over the channel, and the received distorted sequence is compared with the original transmitted one to obtain the channel impulse response used for later equalization. Those equalizers can be either linear or non-linear equalizers in their type.

3.3.1 Linear Equalization

Equalization is linear if it allows estimation of each symbol independently of others. The general idea behind any linear equalization is that the present and the past values of the received signals are linearly weighted by the filter coefficients and summed up to produce the output. It has a finite impulse response (FIR) of length N and its transfer function is [24], [25]:

$$H_{eq} = \sum_{k=0}^{N} w_k z^{-k} \tag{3.6}$$

Also linear equalization process consists of determining coefficients w_k for a known frequency response of the channel, and then updating these coefficients if the channel varies in time. In this section some of linear equalization techniques are discussed.

3.3.1.1 Zero Forcing Equalizer

ZF equalizer is a linear equalization algorithm that simply inverts the complete filter in order to remove any ISI. It applies the inverse of the channel to the received signal, to restore the signal before the channel. Its name ZF corresponds to bringing down the ISI to zero in a noise free environment [26], [24].

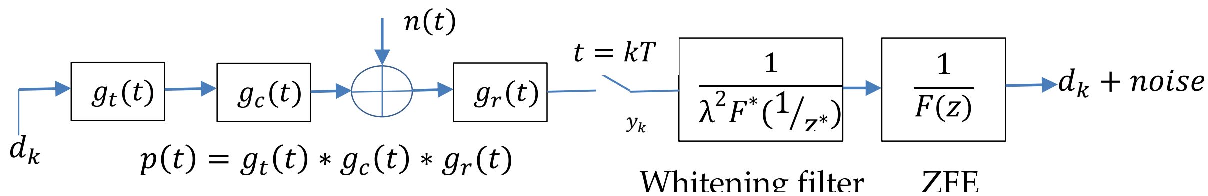

Figure 3.3: ZF equalizer [27]

Using z-transform, the samples entering the equalizer can be represented as follows [27]:

$$D(z)F(z) + U(z) \tag{3.7}$$

Since the transmitted symbols are $d(t) = \sum_{k=-\infty}^{\infty} \mathrm{d_k}\, \delta(\mathrm{t} - \mathrm{kT})$, their z transform is $D(z) = \sum_{k=-\infty}^{\infty} \mathrm{d_k}\, z^{-k}$. Similarly, $U(Z)$ is the z transform of the noise samples, and $F(z)$ is the transfer function of the complete filter after noise has been whitened. The transfer function of the equalizer consequently is [27]:

$$H_{ZF}(z) = \frac{1}{F(z)} \tag{3.8}$$

The signal at the output of the equalizer is $D(z) + H_{ZF}(z)U(z)$, at time kT, the output signal is $d_k + \tilde{u}_k$, where the noise filtered by the equalizer is $\tilde{u}_k$. Consequently, the denoised sample at time kT is equal to the transmitted symbol, and the total equalizer can be seen as the aggregation of the whitening filter and $H_{ZF}(z)$. It is thus equal to [27]:

$$H_{ZF}(z) = \frac{1}{\lambda^2 F^*(\frac{1}{z^*})F(z)} = \frac{1}{P(z)} \tag{3.9}$$

Hence, ZF minimizes the distortion generated by the channel by removing ISI. Yet, since the channel's filter $P(z)$ is an FIR filter, $H_{ZF}(z)$ is Infinite Impulse Response (IIR) filter that cannot be implemented in practice. Moreover, it can also be unstable as its poles can be outside of the unit circle. Consequently, Finite Impulse response (FIR) approximation of this filter must be determined. For this purpose, the FIR filter $H_{\mathrm{eq}}(z) = \sum_{k=0}^{N} w_k z^{-k}$ that minimizes the following distance must obtain [27]:

$$\left| \frac{1}{F(z)} - \sum_{k=0}^{N} w_k z^{-k} \right|^2 \tag{3.10}$$

At this filter's output, some ISIs will not be removed because of this approximation. Another major issue of ZF equalizers is that they may highly increase the noise power spectrum density in some frequency bands. This kind of equalization produces noise enhancement in the spectral nulls due to the form of the transfer function of the equalizer

3.3.1.2 Minimum Mean Squared Error Equalizer

As it is discussed earlier, ZF equalizer neglects the effect of noise. A more robust equalizer is proposed based on the MMSE criterion that aims at minimizing the mean square error between any transmitted symbol d_k and its estimate at the output of the equalizer $\tilde{d}_k$. Its block diagram is shown in Figure 3.3 below.

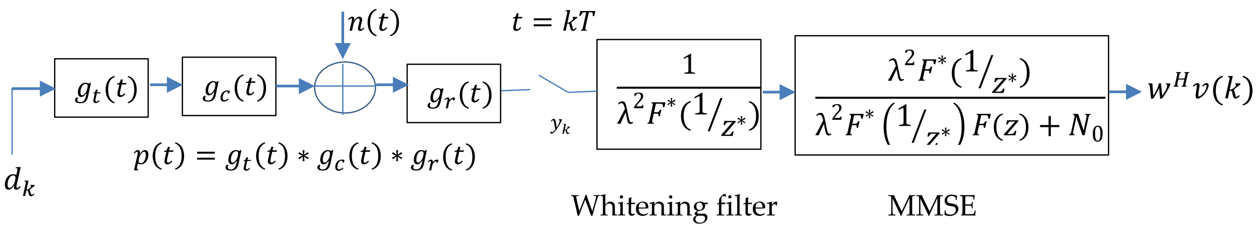

Figure 3.4: MMSE equalizer [27]

We consider the samples v_k at the output of the chain including the whitening filter, given by $v_k = f_0 d_k + \sum_{n=1}^{L-1} f_n d_{k-n} + u_k$. Where $\boldsymbol{f} = [f_k]\ 0 \le k \ll L-1$ is the impulse response of $F(z)$ and u_k is whitened noise. They enter into the filter [27]

$$H_{\mathrm{MMSE}}(z) = \sum_{i=0}^{N} w_i z^{-i} \tag{3.11}$$

The output samples are then estimated. A delay τ may be included. The estimated samples are [27]:

$$\tilde{d}_{k-\tau} = \sum_{i=0}^{N} w_i v_{k-i} = \boldsymbol{w}^H \boldsymbol{V}(k) \tag{3.12}$$

where H stands for the Hermitian operator, which transposes the vector and conjugates all its elements. The complex conjugate vector of the filter's impulse response is denoted as $\boldsymbol{w}^H = [w_0{}^*, w_1{}^*, \dots, w_N{}^*]$. $\boldsymbol{V}(k) = [v_k, v_{k-1}, \dots, v_{k-N}]^T$is the vector of received samples. The mean square error is [27]:

$$
\begin{aligned}
J &= E[|\boldsymbol{w}^H \boldsymbol{V}(k) - d_{k-\tau}|^2] \\
&= \boldsymbol{w}^H E[\boldsymbol{V}(k)\boldsymbol{V}(k)^H]\, \boldsymbol{w} - \boldsymbol{w}^H E[v(k) d^*{}_{k-\tau}] - E[d_{k-\tau}\boldsymbol{V}(k)^H]\, \boldsymbol{w} \\
&\quad + E[|c_{k-\tau}|^2] \\
&= \boldsymbol{w}^H \boldsymbol{R} \boldsymbol{w} - \boldsymbol{r}^H \boldsymbol{w} - \boldsymbol{w}^H \boldsymbol{r} + E[|d_{k-\tau}|^2]
\end{aligned}
\tag{3.13}
$$

$\boldsymbol{R} = E[\boldsymbol{V}(k)\boldsymbol{V}(k)^H]$ is the autocorrelation matrix of the samples at the equalizer's input and $\boldsymbol{r} = E[v(k) d^*{}_{k-\tau}]$ is the cross-correlation vector between samples at the input of the equalizer and the transmitted symbol $d_{\mathrm{k}-\tau}$.

Mean square error is minimized when vector **w** sets the derivative of J with respect to $\boldsymbol{w}^* = [w_0, w_1, \dots, w_N]^T$to zero [27]:

$$
\frac{\partial J}{\partial\, \boldsymbol{w}^*} = -\boldsymbol{r} + \boldsymbol{R}\boldsymbol{w} \tag{3.14}
$$

where the following properties of differential calculus have been used [27]:

$$
\frac{\partial \boldsymbol{r}^h \boldsymbol{w}}{\partial\, \boldsymbol{w}^*} = 0, \qquad \frac{\partial \boldsymbol{w}^H \boldsymbol{r}}{\partial\, \boldsymbol{w}^*} = r, \qquad \frac{\partial \boldsymbol{w}^H \boldsymbol{R} \boldsymbol{w}}{\partial\, \boldsymbol{w}^*} = \boldsymbol{R}\boldsymbol{w} \tag{3.15}
$$

$\frac{\partial J}{\partial\, \boldsymbol{w}^*} = 0$, implies that:

$$
\boldsymbol{w} = \boldsymbol{R}^{-1} \boldsymbol{r} \tag{3.16}
$$

The minimum mean square error is then equal to [27]:

$$J_{min} = E[|d_{k-\tau}|^2] - \boldsymbol{r}^H \boldsymbol{R} \boldsymbol{r} = E_s - \boldsymbol{r}^H \boldsymbol{R} \boldsymbol{r} \tag{3.17}$$

Moreover, it can be shown that if the equalizer has an infinite length [27], then the z transform of $H_{\text{MMSE}}(z)$ is [27]:

$$H_{\text{MMSE}}(z) = \frac{\lambda^2 F^*(1/_{z^*})}{\lambda^2 F(z) F^*(1/_{z^*}) + N_0/_{E_s}} \tag{3.18}$$

The complete equalizer that applies to samples y_k is the product of the whitening filter, $1/\lambda^2 F(z) F^*(1/_{z^*})$ and $H_{\text{MMSE}}(z)$. It is consequently equal to [27]:

$$H_{\text{MMSE}}(z) = \frac{1}{\lambda^2 F(z) F^*(1/_{z^*}) + N_0/_{E_s}} = \frac{1}{P(z) + N_0/_{E_s}} \tag{3.19}$$

The MMSE equalizer has a transfer function quite similar to ZF equalizer, but it takes the noise into account. They become equal if there is no noise term.

3.3.1.3 Least Mean Squared Equalizer

LMS algorithm is the simplest algorithm which is based on minimization of the mean square error between the desired equalizer output and the actual equalizer output. It is a more general approach to automatic synthesis. Instead of solving a set of N simultaneous equations as was done in the ZF and MMSE schemes, the coefficients are gradually adjusted to converge to a filter that minimizes the error between the equalized signal and the stored reference [28].

In practice, the minimization of the mean square error is carried out recursively, and may be performed by use of the stochastic gradient algorithm. It is the simplest equalization algorithm and requires only $2\mathrm{N} + 1$ operations per iteration where N is the length of equalizer weights. Then the filter weights are updated by the update equation. Letting the variable n denote the sequence of iteration, LMS is computed iteratively by [28]

$$w_k(n+1) = w_k(n) + \mu e_k(n) x(n-k) \tag{3.20}$$

where the subscript k denotes the k^{th} delay stage in the equalizer and μ is the step size which controls the convergence rate and stability of the algorithm.

The LMS equalizer maximizes the signal to distortion ratio at its output within the constraints of the equalizer filter length. The convergence rate of the LMS algorithm is slow due to the fact that there is only one parameter, the step size that controls the adaptation rate. To prevent the adaptation from becoming unstable, the value of μ is chosen from [5]

$$0 < \mu < \frac{1}{\lambda_{max}} \tag{3.21}$$

where λ_{max} is the largest eigenvalue of correlation matrix R.

The choice of step size μ ensures that the mean value of the coefficient vector approaches the optimum coefficient vector w_0. It should be mentioned that if the matrix R has a large eigenvalue spread, it is advisable to choose a value for μ much smaller than the upper bound. As a result, the convergence speed of the coefficients will be primarily dependent on the value of the smallest eigenvalue. Implementation of this algorithm can be summarized as the following steps where $d(n)$ stands for desired signal and p for length of equalizer taps [29].

1. Initialization. Set $$\mathrm{w}_k(1) = 0, for\ k = 1,2,\dots,p\ \&\ 0 < \mu < \frac{1}{\lambda_{\max}}$$ 2. Filtering. For time $n = 1, 2, \dots, \&\ k = 1,2,\dots,p$, compute • The estimation of x(n) as: $\hat{x}(n) = \sum_{j=1}^{p} \mathrm{w}_j(\mathrm{n})\mathrm{x}_j(\mathrm{n})$ • The error between $d(n)$ and $\hat{x}(n)$: $\mathrm{e(n)} = \mathrm{d(n)} - \hat{x}(n)$ • Update the filter coefficients: $\mathrm{w}_k(\mathrm{n}+1) = \mathrm{w}_k(\mathrm{n}) + 2\mu\mathrm{e(n)}\mathrm{x}_k(\mathrm{n})$

Table 3.1: Summary of LMS algorithm [30]

3.3.1.4 Recursive Least Square Equalizer

The RLS equalizer is a linear adaptive equalization technique which is based on the method of least squares criteria. According to this method a cost function or index of performance that is defined as the sum of weighted error squares is minimized. In the derivation of the RLS, the input signals are considered deterministic, while for the LMS they were considered stochastic. Derivation of the conventional RLS algorithm relies on a basic result in linear algebra known as the matrix inversion lemma, as it is formulated as follows [4], [31].

Suppose the vectors $Y(i), i = 0,1,\dots,n,$ are observed and the coefficient vectors $h(n)$ of the equalizer that minimizes the time-average weighted squared error are going to be determined [4]

$$\varepsilon^{LS} = \sum_{i=0}^{n} \lambda^{n-i} |e(i)|^2 \tag{3.22}$$

where the error is defined as [4]:

$$e(n) = x(n) - \hat{x}(n) = x(n) - h^T(n)y(n) \qquad (3.23)$$

And λ represents a weighting factor $0 \leq \lambda \leq 1$. Thus exponential forgetting factor is introduced in to the past data, which is appropriate when the channel characteristics are time-variant. Minimization of ε^{LS} with respect to the coefficient vector $h(n)$ yields the following set of equations [4].

$$\frac{\partial \varepsilon^{LS}}{\partial h(n)} = -2\sum_{\mathrm{i}=0}^{\mathrm{n}} \lambda^{\mathrm{n-i}} e(i)y(i) \ = 0$$

$$\frac{\partial \varepsilon^{LS}}{\partial h(n)} = -2\sum_{\mathrm{i}=0}^{\mathrm{n}} \lambda^{\mathrm{n-i}} (x(n) - h^T(n)y(i))y(i) \ = 0$$

$$=> \sum_{\mathrm{i}=0}^{\mathrm{n}} \lambda^{\mathrm{n-i}} x(n)y(i) = \sum_{i=0}^{n} \lambda^{\mathrm{n-i}} y(i)y(i)^T h(n)$$

This can be casted in to the following two defined forms [4].

$$R_{yy}(n) = \sum_{i=0}^{n} \lambda^{\mathrm{n-i}} y(i)y(i)^{\mathrm{T}} \qquad (3.24)$$

$$\mathbf{r_{xy}}(n) = \sum_{i=0}^{n} \lambda^{\mathrm{n-i}} \mathrm{x(n)} y(i) \qquad (3.25)$$

$$=> \mathbf{r_{xy}}(n) = R_{yy}(n)h(n) \qquad (3.26)$$

The solution of Eq. (3.26) will be [4];

$$h(n) \ = {R_{yy}}^{-1}(n)\mathbf{r_{xy}}(n) \qquad (3.27)$$

The matrix $R_{yy}(n)$ is the statistical autocorrelation matrix, while $\mathbf{r_{xy}}(n)$ is the cross-correlation vector. For small values of t, $R_{yy}(n)$ may be conditioned; hence, it is customary to initially add the matrix δx(n) to $R_{yy}(n)$, where δ is a small positive constant and I is the identity matrix [4].

Now suppose the solution of Eq. (3.27) is obtained for time index $n-1$, i.e., $h(n-1)$, and wanted to compute $h(n)$. It is inefficient and impractical to solve the set of N linear equation for each new signal component that is received. To avoid this, it is better to proceed as follows.

First $R_{yy}(n)$ may be computed recursively as [4]

$$R_{yy}(n) = \lambda R_{yy}(n-1) + y^*(n)y(n)^{\mathrm{T}} \tag{3.28}$$

It is called time-updating equation for $R_{yy}(n)$. Since the inverse of $R_{yy}(n)$ is needed in Eq. (3.27), the matrix inverse identity can be used. If $A = R_{yy}(n), B^{-1} = \lambda R_{yy}(n-1), C = y(n), D = 1$, then using the matrix lemma [4];

$$A^{-1} = (B^{-1} + CD^{-1}C^T)^{-1} = B - B(D + C^T BC)^{-1}C^T B \tag{3.29}$$

Then substituting the above definitions into Eq. (3.28), the recursive expression of the inverse autocorrelation matrix can be obtained as follows [4].

$$R_{yy}{}^{-1}(n) = \frac{1}{\lambda}\left[R_{yy}{}^{-1}(n-1) - \frac{R_{yy}{}^{-1}(n-1)y^*(n)y(n)^{\mathrm{T}}R_{yy}{}^{-1}(n-1)}{\lambda + y(n)^{\mathrm{T}}R_{yy}{}^{-1}(n-1)y^*(n)}\right] \tag{3.30}$$

For convenience, let $P(n) = R_{yy}{}^{-1}(n)$. it is also convenient to define an N −dimensional vector, called the Kalman vector, as [4]:

$$K(t) = \frac{1}{\lambda + \mu(n)}P(n-1)y^*(n) \tag{3.31}$$

where, $\mu(n)$ is a scalar defined by [4];

$$\mu(n) = y(n)^{\mathrm{T}} {R_{yy}}^{-1}(n-1)y^*(n) \tag{3.32}$$

With those definitions in Eq. (3.30) becomes [4],

$$P(n) = \frac{1}{\lambda}[P(n-1) - K(n)y^T(n)P(n-1)] \tag{3.33}$$

Suppose both sides of Eq. (3.33) are post multiplied by $y^*(n)$ [4]

$$P(n)y^*(n) = \frac{1}{\lambda}[P(n-1)y^*(n) - K(n)y^T(n)P(n-1)y^*(n)]$$

$$= \frac{1}{\lambda}\{[\lambda + \mu(n)]K(n) - K(n)\mu(n)\} = K(n) \tag{3.34}$$

Therefore, the Kalman gain vector can be defined as $P(n)y^*(n)$. Now using the matrix inversion identity to derive an equation for obtaining $h(n)$ from $h(n-1)$. Since $h(n) = P(n)\boldsymbol{r_{xy}}(n)$ and [4]

$$\boldsymbol{r_{xy}}(n) = \lambda \boldsymbol{r_{Iy}}(n-1) + \mathrm{x(n)}\boldsymbol{y}^*(n) \tag{3.35}$$

This will result in [4]

$$h(n) = \frac{1}{\lambda}[P(n-1) - K(n)y^T(n)P(n-1)]\left[\lambda \boldsymbol{r_{xy}}(n-1) + \mathrm{x(n)}\boldsymbol{y}^*(n)\right]$$

$$= P(n-1)\boldsymbol{r_{xy}}(n-1) + \frac{1}{\lambda}\,\mathrm{x(n)}\boldsymbol{y}^*(n)P(n-1) - K(n)y^T(n)P(n-1)\boldsymbol{r_{xy}}(n-1)$$
$$- \frac{1}{\lambda}\mathrm{x(n)}K(n)y^T(n)P(n-1)\boldsymbol{y}^*(n)$$

$$h(n) = h(n-1) + K(n)[\mathrm{x(n)} - y^T(n)h(n-1)] \tag{3.36}$$

Hence $y^T(n)h(n-1)$ is the output of the equalizer at time n therefore [4];

$$\hat{\mathrm{x}}(\mathrm{n}) = y^T(n)h(n-1) \tag{3.37}$$

And,

$$e(n, n-1) = \mathrm{x(n)} - \hat{\mathrm{x}}(\mathrm{n}) = e(n) \tag{3.38}$$

where, $e(n)$ is the error between the desired symbol and the estimate.

Hence $h(n)$ is updated recursively according to the following relation [4].

$$h(n) = h(n-1) + K(n)e(n) \tag{3.39}$$

The residual MSE resulting from this optimization becomes [4]

$$\varepsilon_{N\,min}{}^{LS} = \sum_{i=0}^{n} \lambda^{n-i}|\mathrm{x(n)}|^2 - h^T(n)\boldsymbol{r_{xy}}^*(n) \tag{3.40}$$

The following table summarizes the steps of RLS algorithm.

1. Initialization. Set $\mathrm{h}(0) = 0, P(0) = \sigma^2 I, \sigma^2 >> 1$, read in the first sample of the input signal vector $X(1) = [x(1) \quad 0 \quad \cdots \quad 0]$
2. In each discrete moment of time k= 1, 2, . . ., assuming that $\mathrm{h}(\mathrm{k}-1), \mathrm{X}(\mathrm{k})$ and $P(k-1)$ are known, calculate:
• Input signal estimation: $\hat{\mathrm{x}}(\mathrm{k}) = y^T(k)h(k-1)$
• Error signal: $e(n) = \mathrm{x(k)} - \hat{\mathrm{x}}(\mathrm{k}) = \mathrm{x(k)} - y^T(k)h(k-1)$
• Kalman gain vector: $K(k) = \frac{1}{\lambda+\mu(k)}P(k-1)y^*(k)$
• The inverse correlation matrix: $P(k) = \frac{1}{\lambda}[P(k-1) - K(k)y^T(k)P(k-1)]$
• Filter coefficients: $h(k) = h(k-1) + K(k)e(k) = h(k-1) + P(k)y^*(k)e(k)$
• Update input vector: $\boldsymbol{X}^T(k+1) = [x(k+1) \;\; x(k) \;\; x(k-1) \;\; \ldots \;\; x(k-M+1)]$
Increment counter k by 1 and repeat the procedure from step 2

Table 3.2: Summary of RLS algorithm[30]

The major advantage of RLS equalizer lies on its fast convergence and good tracking abilities. But its complexity is higher compared to the LMS equalizer [4].

3.3.2 Non-Linear Equalization

Non-linear equalization is needed when the channel distortion is too severe for linear equalizers to mitigate. For such channels which have deep spectral nulls in the pass band, non-linear equalizers can be used to compensate the channel impairments by placing too much gain in the vicinity of the spectral null [13]. Two of the most common types of non-linear equalization techniques are described below.

3.3.2.1 Decision Feedback Equalizer

The DFE is a non-linear equalizer that uses the channel impulse response, as well as previous decision, to eliminate the ISI of the future samples. As shown in Figure 3.5 below, the DFE consists of a feedforward filter W(z) with the received sequence as input (similar to the linear equalizer) followed by a feedback filter V(z) with the previously detected sequence as input. In effect, the DFE determines the ISI contribution from the detected symbols $\{\hat{\hat{d}}\}$ by passing them through a feedback filter that approximates the composite channel F(z) convolved with the feedforward filter W(z). The resulting ISI is then subtracted from the incoming symbols. Since the feedback filter V(z) in Figure 3.5 sits in a feedback loop, it must be strictly causal or else the system is unstable. The feedback filter of the DFE does not suffer from noise enhancement because it estimates the channel frequency response rather than its inverse [12].

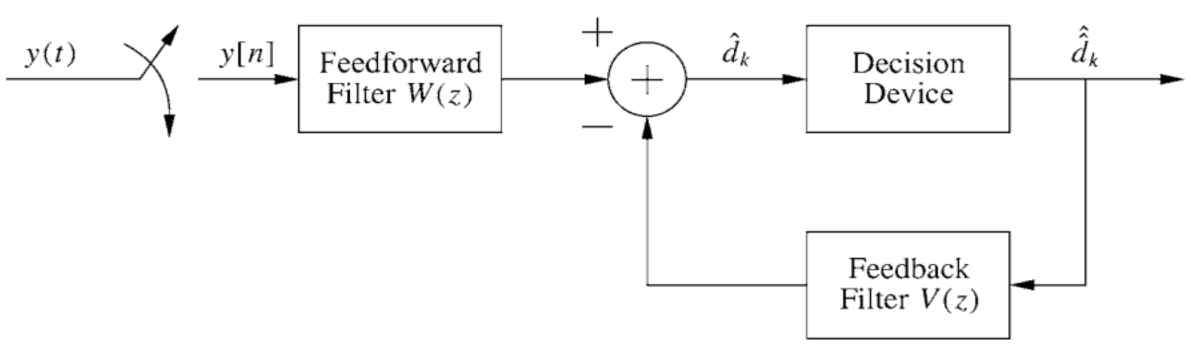

Figure 3.5: DFE structure [12]

Assuming $W(z)$ has $N_1 + 1$ taps and $V(z)$ has N_2 taps, the DFE output can be written as [13]:

$$\hat{d} = \sum_{i=-N_1}^{0} w_i y[k-i] - \sum_{i=1}^{N_2} v_i \hat{\hat{d}}_{k-i} \tag{3.41}$$

The algorithm for selecting the coefficients for $W(z)$ and $V(z)$ can be ZF, MMSE, LMS or RLS based on the required minimization criteria.

The advantage of a DFE implementation is the feedback filter, which is additionally working to remove ISI, and thus eliminates additive noise from the feedback signal. However, it exhibits feedback errors if $\hat{\hat{d}} \neq \hat{d}$, since the ISI subtracted from the feedback path is not the true ISI corresponding to d_k. Such errors therefore propagate to later bit decisions leading to error propagation. In other words if the reciever takes a wrong decision for one bit, then the later computed ISI will be erroneous too, and the future samples arriving to the receiver will be even more affected by ISI than unequalized ones. Moreover, this error propagation cannot be improved through channel coding, since the feedback path operates on coded channel symbols before decoding. This is because the ISI must be subtracted immediately, which doesn't allow for any decoding delay. Hence the error propagation seriously degrades performance DFE specially on channels with low SNR [12].

3.3.2.2 Maximum Likelihood Sequence Estimation Equalizer

MLSE equalizer directly estimates the sequences of transmitted symbols from received sequences of interfered and noisy symbols. Consequently, this type of equalization does not increase the noise power. In this technique equalization is no longer performed per symbol, but for a sequence of symbols in this case.

At the input of MLSE, a whitening filter ${}^{1}\Big/_{(\lambda^2 F^*({}^{1}/_{z^*}))}$ is used to whiten the noise. The equivalent channel before equalization consequently is $F(z)$. Let us assume that the channel's impulse response generates L ISI terms. Its z transform is then: $F\,(z) = \sum_{n=0}^{L-1} f_n z^{-n}$ .The transmitted symbols, denoted as c_k, belong to an M-symbols modulation whose elements are located in set C [12].

Let us assume that N interfered and noisy symbols $\mathbf{V} = [v_0, v_1, \dots, v_{N-1}]$ are received. The noise samples, $\mathbf{u} = [u_0, u_1, \dots, u_{N-1}]$, are i.e., white due to the whitening filter, and of variance $\sigma^2 = N_0/2$.

The probability to receive $\mathbf{V} = [v_0, v_1, \dots, v_{N-1}]$ knowing that $\mathbf{C}$ was transmitted depends on the probability density of noise $u_k = v_k - \sum_{m=0}^{L-1} f_m c_{k-m}$ on each element k of the sequence. Since the noise samples are independent, it is equal to [27]:

$$p(\boldsymbol{V}/\boldsymbol{C}) = \prod_{k=0}^{N-1} \frac{1}{\sqrt{\pi N_0}} \exp\left\{-\frac{|v_k - \sum_{m=0}^{L-1} f_m c_{k-m}|^2}{N_0}\right\}$$

$$= \left(\frac{1}{\sqrt{\pi N_0}}\right)^N \exp\left\{-\frac{1}{N_0}\sum_{k=0}^{N-1}\left|v_k - \sum_{m=0}^{L-1} f_m c_{k-m}\right|^2\right\} \tag{3.42}$$

The optimum estimated transmitted sequence according to the ML criterion is consequently defined as follows [27]:

$$\hat{\mathbf{C}} = \arg\max_{c\in C^N}\left(\frac{1}{\sqrt{\pi N_0}}\right)^N \exp\left\{-\frac{1}{N_0}\sum_{k=0}^{N-1}\left|v_k - \sum_{m=0}^{L-1} f_m c_{k-m}\right|^2\right\} \tag{3.43}$$

To simplify the previous objective, it is preferable to study the log-likelihood [27]:

$$\hat{\mathbf{C}} = \arg\max_{c\in C^N}\left(-\sum_{k=0}^{N-1}\left|v_k - \sum_{m=0}^{L-1} f_m c_{k-m}\right|^2\right) \tag{3.44}$$
$$= \arg\min_{c\in C^N}\left(\sum_{k=0}^{N-1}\left|v_k - \sum_{m=0}^{L-1} f_m c_{k-m}\right|^2\right)$$

It can be noted that for any given sequence $\boldsymbol{c}, d_k = \sum_{m=0}^{L-1} f_m c_{k-m}$ depends on $[c_k, c_{k-1}, \ldots, c_{k-L+1}]$. The received signal at time $k+1, d_{k+1}$ depends on $[c_{k+1}, c_k, c_{k-1}, \ldots, c_{k-L+2}]$.

Since $c_{\mathrm{k+1}}$ belongs to M symbols modulation, there are M possible paths to pass from d_k to d_{k+1}. In order to determine c_{k+1}, a trellis with M input paths and M output paths can be built. This trellis will contain M^L states since L symbols that can take M values are stored in shift registers. The transmit symbols sequence can then be obtained by applying Viterbi's algorithm on this trellis. Looking for the most likely sequence is equivalent to determining the most likely path in the trellis, knowing the received sequence symbols and the channel's impulse response. Thus, Viterbi's algorithm must be applied on the received symbols using the squared Euclidean distance for branches metrics, $|v_k - \sum_{m=0}^{L-1} f_m c_{k-m}|^2$. To simplify the computation, the absolute value metric $|v_k - \sum_{m=0}^{L-1} f_m c_{k-m}|$ is often used instead of the squared Euclidean distance [12].

The best advantage of MLSE equalizer is minimization of BER compared to all other structures; however the computation effort needed for this equalizer increases exponentially with length of the sequences length making it not acceptable for a practical implementations [12].

Chapter Four

End to End Communication System Model

4.1 End to End System Block Diagram

Figure 4.1 below shows the end to end communication system model used for simulation in this thesis work. It starts from the data generation phase to the input processing, gray coding and digital modulation process in the transmitter part. Those generated symbols are then passed through a random channel and the reception process follows. In the receiver part it shows the counter part of the signal processing blocks used in the transmitter part like digital demodulation, gray decoding, equalization, digital to analog conversion and information sink. Descriptions of each block are presented in the next sub-sections.

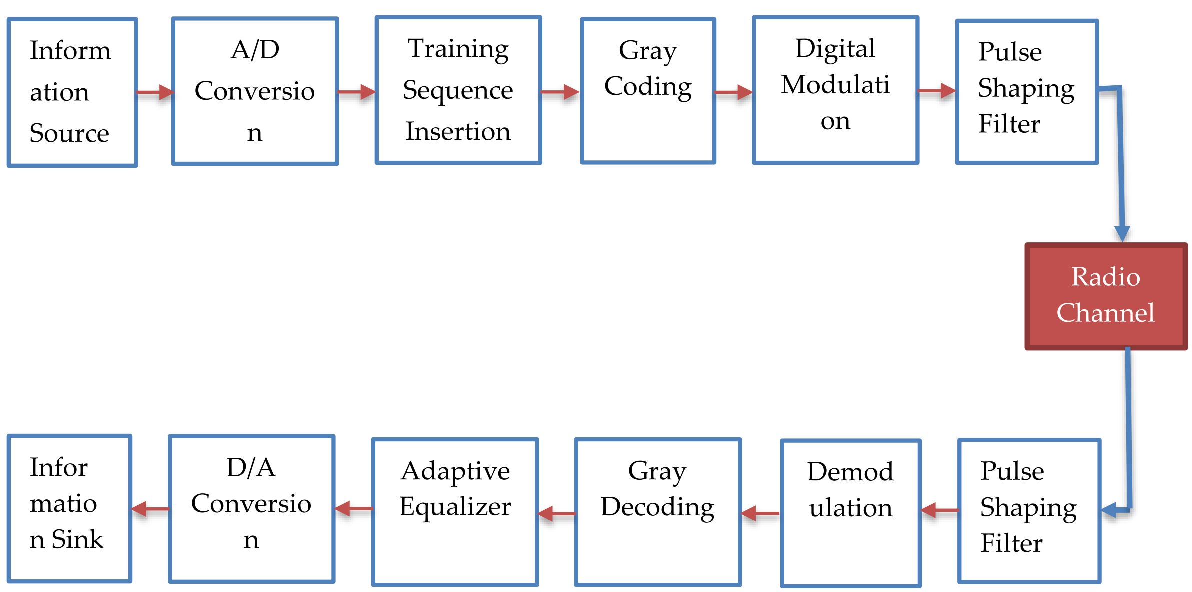

Figure 4.1: Simulation block diagram

The block diagram shows only the basic functional blocks implemented for simulation in the next Chapter. Modern broadcast system implementations may add some additional blocks such as further bit stream processing and encapsulation techniques like MPEG in the transmitter. Also broadcast systems like DVB-T2 use powerful coding schemes based on the combination of Low Density Parity Check (LDPC) and Bose-Chaudhuri-Hocquenghem (BCH) error correcting codes as well as a combination of bit, cell, time and frequency interleaving techniques [32], [33]. This thesis concentrates only on the basic functional blocks in single frequency applications by skipping those detailed signal processing blocks.

4.2 Block Diagram Description

The next sections present the functional blocks in the transmitter, channel and receiver blocks.

4.1.1 Transmitter Block

As shown in the block diagram above, the transmitter block includes the input generation and processing, pilot (training) sequence insertion, channel coding and modulation processes. Each functional blocks are described as follows.

4.1.1.1 Input Generation and Processing

The input to this model can be analog signal either in the form of sound, image or video signal. In such cases, analog to digital convertor is used to convert the analog input signal into continuous bit streams by sampling the input based on the Nyquist criteria. After this block, the input signal is converted in to digital form and it is treated as binary code in the rest of blocks. The digital to analog converter in the receiver performs the inverse of this block by converting the received signal back to its original form.

In this case, the input generator is designed to support two types of source data, either a randomly produced data or an image file. The random data is ideal to test the channel impact to the BER performance of the reception. On the other hand image file can give an intuitive visual impression and comparison for different channels. As a result, the random signal is used in every BER performance simulations while the image signal is used for constellation plot and image quality comparison before and after equalization.

4.1.1.2 Training Sequence Generation and Pilot Insertion Techniques

After the source data is produced, the pilot data is inserted into head of source data in each coherence time. These training sequence is generated by using a random integer generator and are used to estimate the random phase shift of the fading channel and train the equalizer to adjust the received signal accordingly. This training sequence is usually selected to be a periodic pseudo-random sequence whose length is selected by taking trade-offs between estimation performance and bandwidth efficacy. For example a GSM system uses 26 bits training sequence out of 148 useful information bits. The training bits are about 17.56% the information bits and the system can be translated to be a waste of bandwidth. To improve the bandwidth efficiency, modern systems like DVB limit the length of training sequence to be 8% of the total bits. The training sequence is also limited to be 8% of the total bits to limit the overhead bits according to the DVB standards [33].

Training sequence arrangements can be either in comb, block or lattice type structures. In comb-type, pilot information is inserted along the frequency axis to estimate the channel response in frequency domain and has ability to tackle the problem of fast fading channel. The occurrence of training symbols is a function of coherence bandwidth, which is related to maximum delay spread a channel can have. For a block-type structure, training sequences are inserted among all the message symbols along the time axis to estimate the channel response in the time domain and have the ability to overcome the problem of frequency selectivity of the channel. This technique is selected for this thesis since its main target is to overcome frequency selectivity of a channel. The occurrence of training symbols is a function of coherence time, which is also related to Doppler shift in the channel. The third one is Lattice-type structure which incorporates both block and comb type techniques and insert training sequence in both frequency and time axis. It exploits both frequency and time domain interpolation techniques for the estimation of varying channel [34].

4.1.2.3 Training Methodology

As it was explained earlier, any training based adaptive algorithm requires knowledge of the desired response to form the error signal needed for equalization. In theory, the transmitted sequence is the desired response for an adaptive equalizer. In practice, the equalizer is physically separated from the transmitter of its ideal desired response since the equalizer is located in the communication receiver. For that reason, there are two methods in which a replica of the desired response can be generated locally in the communication receiver: training only and decision directed methods [17].

4.1.2.3.1 Training Only Method

This method is used during the initial training phase that takes place when the communication transmitter and receiver first establish a connection. A replica of the desired response is used from the signal sequence $d(n)$, when the transmitter sends a sequence that is known to the receiver. In fact, the generator of such a reference signal must be synchronized with the known transmitted sequence. In addition, Haykin [35] suggested using a test signal containing a pseudo-noise sequence with a broad and even power spectrum because the pseudo-noise sequence has noise-like properties and a periodically deterministic waveform.

4.1.2.3.2 Decision-Directed Method

This method is to use the output sequence $y(n)$ of the threshold device in the receiver as the transmitter sequence during the normal operation. Accordingly, if the output $y(n)$ is the correct transmitted sequence, then it may be used as the desired response to form the error sequence for the purpose of the adaptive equalizer. This method is said to be decision-directed because it is based on the decisions made by the communication receiver. Generally, for high performance equalization, it is recommended that an adaptive equalizer be trained before it is switched to the decision directed method [9].

4.1.1.3 Gray Coding

In most cases, the one-to-one mapping of N-bit sequences to 2^N levels is arbitrary. The most straightforward coding technique is to use a natural binary code. However, the mapping where the bits assigned to the two neighboring levels differ only by one bit is called Gray coding. This property is advantageous in a multilevel transmission system where decision errors occur mostly between two neighboring levels; a symbol error results in a one-bit error in this case, while it may cause a two-bit error or more when a natural binary code is used. For that reason gray coding technique was chosen in this model over the natural coding technique or the likes of on-off, polar and split-phase codes that can be used in unipolar line coding cases [23].

If a 2^N-level $(N \geq 2)$ system was considered and the bit patterns are expressed as $(a_{n-1}, a_{n-2}, a_{n-3}, \dots, a_0)$ for the natural binary code and $(b_{n-1}, b_{n-2}, b_{n-3}, \dots, b_0)$ for the gray code, the gray code is generated such that [23]

$$b_{n-1} = a_{n-1}$$

$$b_i = a_{i+1} \oplus a_i \quad (i = n-2, n-3, n-4, \dots, 0) \tag{4.1}$$

where $\oplus$ denotes the modulo 2 addition, that is, $0 \oplus 0 = 0, 0 \oplus 1 = 1, 1 \oplus 0 = 1,$ and $1 \oplus 1 = 0$. After gray coding, data is mapped from binary data to complex data, and each output datum represents a point in the constellation diagram [23].

4.1.1.4 Modulation Process

The modulation process by which a carrier wave is made to carry the message or digital signal is next, and a choice can be made between different modulation schemes allowing trade-off between transmission data rates and signal robustness. The basic modulation methods include: amplitude, frequency and phase shift keying. Amplitude and phase modulations can also be combined to give QAM. Higher order modulation schemes are more bandwidth efficient than their lower order counterparts. However, this bandwidth efficiency is usually obtained at the cost of reduced power efficiency or signal robustness. Hence the selection criteria in this thesis work is a modulation technique which can provide certain BER performance relatively with affordable price in power requirement and simpler implementation complexity. The BER performance comparison of M-PSK and M-QAM techniques was carried out in [36], and the results discussed in this paper for the cases of LMS and RLS equalizers are presented in Section (4.1.3.1) of this Chapter.

4.1.1.5 Pulse Shaping Filter

Communication systems, which operate with the minimum bandwidth, have not only ISI effects but also out-of-band radiation. Thus, it is highly desirable to reduce modulation bandwidth and suppress the out-of-band radiation while eliminating the ISI simultaneously. Pulse shaping filter is used as one of the technique to reduce the ISI effects at sampling instance and spectral width of a modulated signal. It is the process of shaping pulses to be transmitted based on the symbols generated via modulation. The goal is to make the signal suitable to be transmitted through the communication channel mainly by limiting its effective bandwidth. There are three pulse shaping options namely: Raised Cosine (RC), Square Root Raised Cosine (SRRC) and Gaussian filters [2].

RC pulse: This is a pulse widely used in practice. The pulse shape and the excess bandwidth can be controlled by changing the roll-off factor ($0 \leq \alpha \leq 1$, where 0 means no excess bandwidth, and 1 means maximum excess bandwidth). The frequency-domain expression of raised-cosine filter is given in (Eq. 4.2) [2], [37];

$$G_{RC}(f) = \begin{cases} T, & 0 \leq |f| \leq \frac{(1-\alpha)}{2T} \\ \frac{T}{2}\left[1 + \cos\frac{\pi T}{\alpha}\left(|f| - \frac{(1-\alpha)}{2T}\right)\right], & \frac{(1-\alpha)}{2T} \leq \frac{(1+\alpha)}{2T} \\ 0, & |f| > \frac{(1+\alpha)}{2T} \end{cases} \tag{4.2}$$

SRRC: The total effective filter of the transmission system is the combination of transmit and receive filter $g_{TX} * g_{RX}$, where $*$ is convolution. This effective filter (and not the individual filters) must fulfill the Nyquist criterion. This goal can be achieved if both filters have a transfer function that is equal to the square root of that of the raised cosine filter. Such a filter is therefore called a SRRC. The combination of both SRRC filters then becomes a raised cosine and thus fulfills the Nyquist criterion. Furthermore, since the filters are real valued and symmetric, the SRRC is its own matched filter [2], [37]. Because of this property of SRRC pulse shaping filter was chosen to be used in the model.

The impulse response of the SRRC filter is given in [37]:

$$G_{SRRC}(f) = \sqrt{G_{RC}(f)} \tag{4.3}$$

Gaussian pulse: The impulse response of this filter is a Gaussian function. Gaussian pulses have good spectral properties (low spectral side lobes). It has the transfer function given by [37]

$$G_G(f) = exp[-(\alpha f)^2] \tag{4.4}$$

where $\alpha = \frac{\sqrt{2\ln 2}}{\beta}$, and β is the 3-dB bandwidth of the baseband shaping filter. The transfer function $G_G(f)$ is a bell shape and symmetric at $f = 0$ [2].

4.1.2 Transmission Channel

In this model, two different channel types, namely: AWGN channel and Rayleigh frequency selective fading channel are used. The AWGN channel is used as a reference to compare the results obtained using frequency selective channel.

4.1.2.1 AWGN Channel Model

AWGN channel is very straightforward by just adding a white Gaussian noise into the transmitted signal to meet a specified SNR value. The assumption of AWGN essentially means that the primary source of the noise is at the receiver or is radiation impinging on the receiver that is independent of the paths over which the signal is being received.

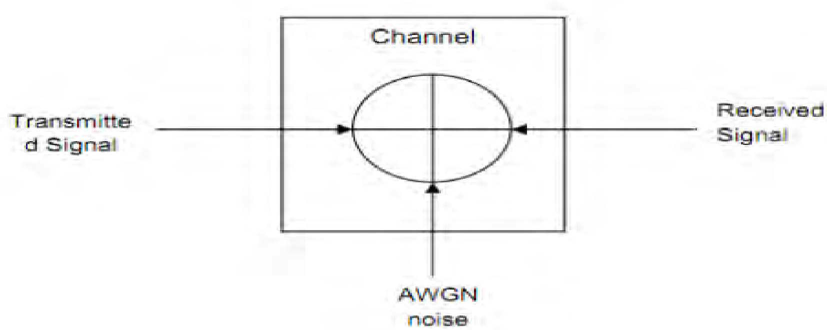

Figure 4.2: AWGN channel model **[38]**

AWGN channel is assumed to have a constant statistical distribution over the channel bandwidth, and a Gaussian amplitude probability density function. It is added to the transmitted signal prior to the reception at the receiver as shown in Figure 4.2 above. The transmitted signal, AWGN and received signal are then expressed by the following equation with s(t), n(t) and r(t) representing those signals respectively [38]:

$$r(t) = s(t) + n(t) \tag{4.5}$$

4.1.2.2 Frequency Selective Channel Model

In this case the COST 207 channel models which are standardized to enable different communication designers to simulate their systems using a common set of channel models in frequency selective environment are used. The standard defines four channel models namely RA, TU, BU, and HT as it is described in Chapter two of this paper. The following table summarizes all the channel parameters of those channel types [22].

Path no. (L)	Propagation delay	Path power (Lin.)	Path power (dB)	Category of the Doppler Spectrum	Delay spread
RU channel					
0	0.0 μs	1	0	"Rice"	0.1 μs
1	0.2 μs	0.63	-2	"Jakes"	
2	0.4 μs	0.1	-10	"Jakes"	
3	0.6 μs	0.01	-20	"Jakes"	
TU channel					
0	0.0 μs	0.5	-3	"Jakes"	1.1 μs
1	0.2 μs	1	0	"Jakes"	
2	0.6 μs	0.63	-2	"Gauss I"	
3	1.6 μs	0.25	-6	"Gauss I"	
4	2.4 μs	0.16	-8	"Gauss II"	
5	5.0 μs	0.1	-10	"Gauss II"	

BU channel					
0	0.0 μs	0.5	-3	"Jakes"	
1	0.4 μs	1	0	"Jakes"	
2	1.0 μs	0.5	-3	"Gauss I"	
3	1.6 μs	0.32	-5	"Gauss I"	2.4 μs
4	5.0 μs	0.63	-2	"Gauss II"	
5	6.6 μs	0.4	-4	"Gauss II"	
HT channel					
0	0.0 μs	1	-3	"Jakes"	
1	0.2 μs	0.63	0	"Jakes"	
2	0.4 μs	0.4	-4	"Jakes"	
3	0.6 μs	0.2	-7	"Jakes"	5.0 μs
4	15.0 μs	0.25	-6	"Gauss II"	
5	17.2 μs	0.06	-12	"Gauss II"	

Table 4.1: Specification of the L-path channel models according to COST 207 [20], [22], where $L = 4$ (RA) and $L = 6$ (TU, BU, HT).

From those models the TU model was standardized to be used in TU environments and in this simulation model it was chosen with 6 paths to represent the frequency selective channel characteristics.

4.1.3 Receiver Block

The receiver block consists of the inverse operations of the combined transmitter and channel effects. Those operations performed in the receiver consists of digital demodulation, channel decoding, trained adaptive equalization and source recovery. In this the section selection criteria of equalization techniques will be discussed.

4.1.3.1 Adaptive Equalization

Since an adaptive equalizer compensates for unknown channel, it requires a specific algorithm to update the equalizer coefficients and track the channel variations. When selecting an equalizer for a practical system, the following criteria have to be considered [1]:

- **Handling zeros in the channel transfer function:** ZF and MMSE equalizers have problems, as they invert the transfer function and thus create poles in the equalizer transfer function. None of the rest equalizers have this problem [39].
- **Sensitivity to channel mis-estimation:** due to the error propagation effect, DFE equalizers are more sensitive to channel estimation errors than linear equalizers. Also, ZF equalizers are more sensitive than MMSE equalizers.
- **Computational effort**: Depending on the adaptation algorithm, the number of operations increases linearly, quadratically, or cubically with equalizer length (number of weights). For DFE equalizers the computational effort increases quadratically while in the case of MLSE, it increases exponentially with length of the impulse response of the channel [39]. Table 4.1 below summarizes the computational complexities of selected algorithms as follows. Here N represents the length of equalizer weights and k stands for length of the input sequence.

Algorithm	Computational Resources				Tracking	Convergence time	Stability
	Memory usage	Multiplications per T_s	Addition	Complexity			
ZF	N^2	N^2	N^2	High	Poor	$\sim NT_s$	Unstable
MMSE	N^2 to N^3	N^2 to N^3	N^2 to N^3	V. High	Poor	$\sim NT_s$	Less stable
LMS	$2N$	$2N+1$	$2N+1$	Low	Poor	$> 10NT_s$	Less stable
RLS	N^2+2N	$2(N^2+2N)$	$1.5N^2+2.5N$	High	Good	$\sim NT_s$	Highly stable
DFE	$20N$	$20N+5$	$20N+5$	High	Good	$\sim NT_s$	Unstable
MLSE	e^K	e^K	e^K	V. High	Good	$\sim NT_s$	Highly stable

Table 4.2: Computational resource requirements and relative convergence speed comparisons for different adaptive filter algorithms [12], [40]

- **Power consumption and cost**: these can be deduced from the computational effort.
- **Minimization of the BER**: here MLSE is superior to all other structures. DFEs, though worse than MLSE estimators, are better than linear equalizers. The quantitative difference between the structures depends on the channel impulse response. The BER performance comparisons of linear and non-linear equalizers are presented in [38] & [41], and BER comparisons between LMS and RLS equalizers are carried out in [36]. The results of journals are presented in the next pages.

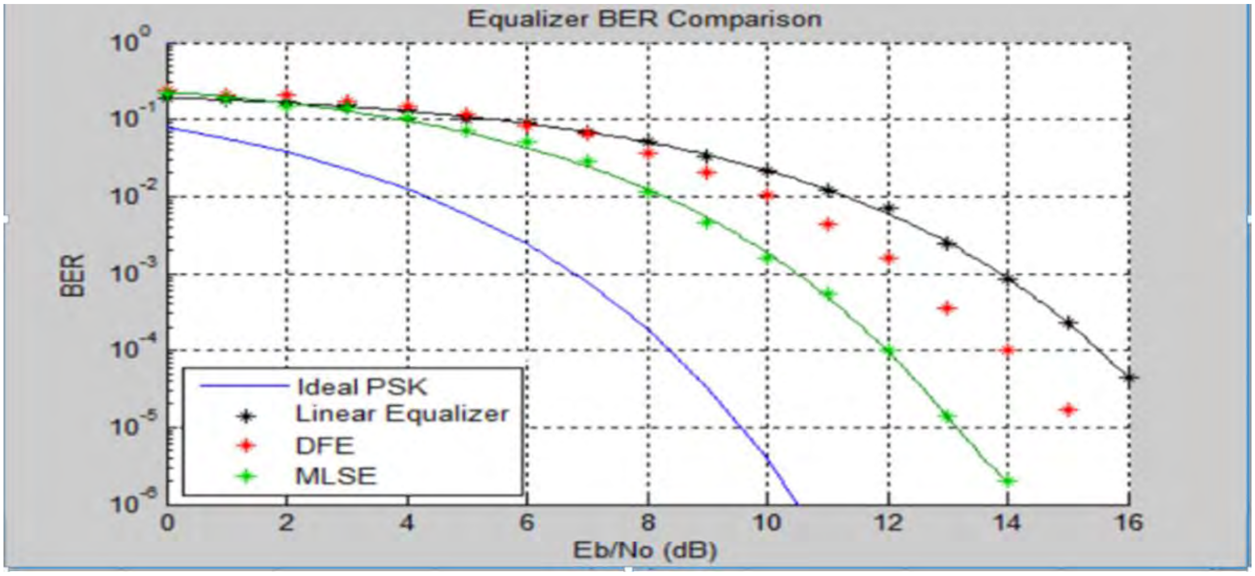

Figure 4.3: BER comparison different equalizers [26], [41]

Figure 4.6 above shows the BER performance comparison of RLS algorithm based linear equalizer with DFE and MLSE based non-linear equalizers. As it is shown in the figure, the MLSE equalizer has the best BER performance against the DFE and RLS equalizers. It tries to follow the performance of ideal PSK in AWGN channel. However, its exponentially growing computational complexity is very high when compared to the rest two techniques. DFE is also slightly better than RLS equalizer by achieving a BER performance of 10^{-4} at 14dB SNR. But still its computational and structural complexity is higher and it also tends to be unstable in the case of estimation errors due to the error propagation phenomena. The RLS equalizer is computationally simpler than the rest two equalizers but still has nearly comparative performance with DFE equalizer. With this equalizer it is possible to achieve a BER performance of 10^{-4} at around 15dB SNR which is sufficient for voice, audio and image reception.

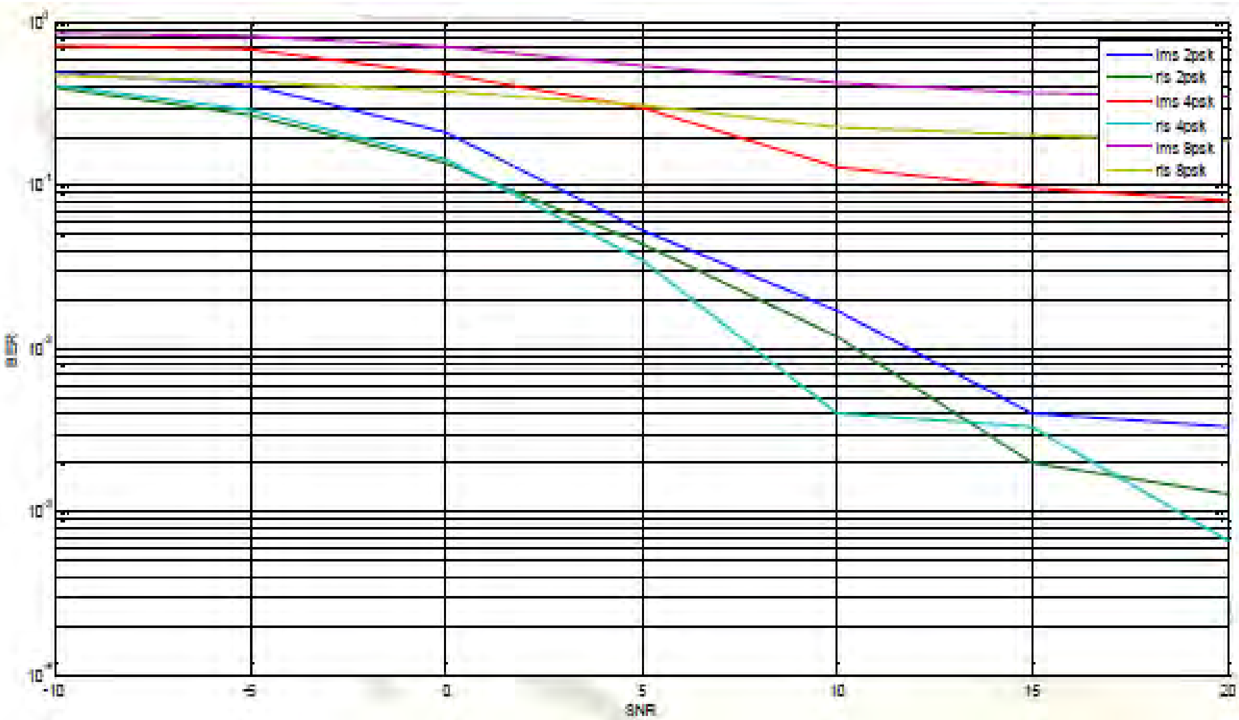

Figure 4.4: BER performance comparison of M-PSK modulation systems using LMS and RLS equalizers [36]

Figure 4.4 shows BER vs SNR performanmce comparison of LMS and RLS equalizers for M-PSK modulation systems. From the figure, it can be observed that the RLS algorithm performs better than LMS algorithm in all binary phase shift keying (BPSK), QPSK and 8-PSK cases. However, when the modulation order increases the BER performance of both systems decreases slowly with increasing SNR. It can also be observed that the performance of RLS equalizer with QPSK modulation is better than LMS system with BPSK modulation and nearly comparable with RLS equalizer with BPSK modulation system while providing double data rate capability than the BPSK system.

Figure 4.5 also shows the BER vs SNR performance comparison of those two equalizers in the case of higher order QAM systems. Here also the RLS equalizer is shown to perform relatively better than its LMS counterpart. However, this BER performance is not good enough for practical applications that require smaller BER performance in which the RLS equalizer in this case failed to attain below 20 dB SNR.

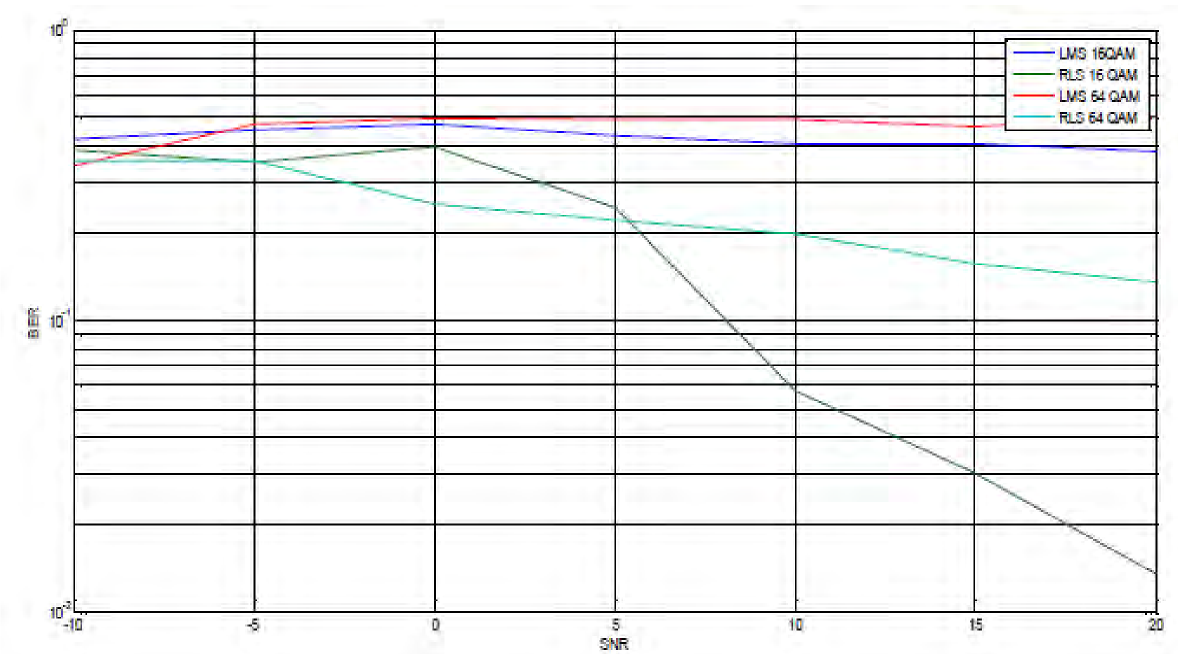

Figure 4.5: BER performance comparison of M-QAM modulation systems using LMS and RLS equalizers [36]

Hence, based on the above results, RLS equalizer with QPSK modulation system was chosen in the model instead of other modulation orders and the LMS algorithm for practical simulation in the next Chapter.

Chapter Five

Simulation Results and Discussions

In this section the simulation setup and descriptions of the results obtained from the simulation task are presented. The chapter consists of the simulation flow chart to illustrate the methods implemented in this simulation together with appropriate parameters used in each block. Then results obtained in AWGN and frequency selective channels are also presented in order.

5.1 Simulation Flow Chart

Figure 5.1 below shows the simulation flow chart of the model used for simulation in this thesis work. It shows the step by step flows of the simulation process starting from the initialization part to the final result presentation.

As it can be seen from the figure, the simulation is designed to support two types of source data, either the randomly produced data or an image file. The random data is used for all BER plots and the image file is used for constellation plot and image quality comparison before and after the equalization process.

Two different channel types namely AWGN channel and AWGN plus Rayleigh frequency selective fading channel are also simulated. AWGN channel is very straightforward by just adding a white Gaussian noise into the transmitted signal to meet a specified SNR value. In the case of frequency selective fading channel which is the main target of this thesis work, the TU6 channel model described in Chapter two is used. The maximum speed of the receiver is set to be $60km/hr$ in TU environment.

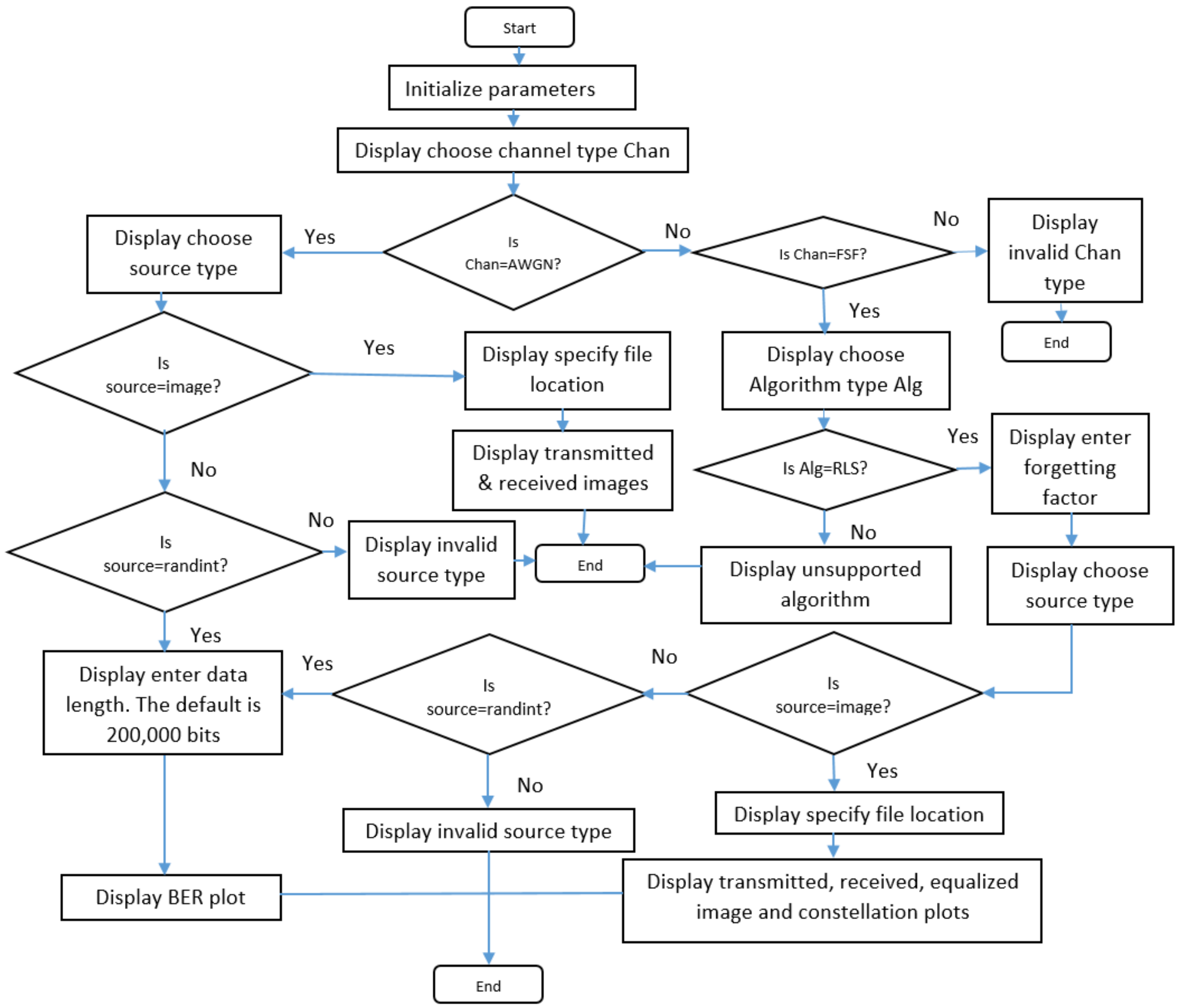

Figure 5.1: Simulation flow chart

In the receiver side, non-blind adaptive equalizer was used to mitigate the effect of frequency selective fading channel by using the RLS algorithm as adaptation mechanism. Since the channel length is 6, the number weights of the RLS equalizer was selected to be 8 which is the smallest power of 2 greater than 6. Another important parameter of this RLS equalizer is its forgetting factor which is usually advised to be a number close to 1. By trial and error the value of this parameter was selected to be 0.99 which minimizes the BER.

5.2 Simulation Parameters

The simulations have been performed using MATLAB software and below are the parameters used in the simulation:

Simulation Parameter	**Values Used**
Equalizer type	Linear
Adaptation Algorithm	RLS
Forgetting Factor	0.99
No of tap-weights	8
Maximum speed of the receiver	60Km/hr.
Source type	Random integer, Image file
Data length	200,000 bits
Length of Training Sequence	8% of the data length
Training methods	Training only, decision directed mode
Modulation techniques	QPSK
Channel model	AWGN, TU6
Channel length	6
SNR	15dB
Operating frequency band	UHF
Carrier frequency	400 MHz
Channel bandwidth	1.9MHz
Doppler shift	22.22 Hz
Coherence bandwidth	182KHz
Symbol rate	0.526μs
Delay spread	1.1 μs
Coherence time	0.0081 s

Table 5.1: Simulation parameters

5.3 Results and Discussions

In this section results of the simulation work are presented together with discussion of each results obtained from the simulation experiment. For the sake of comparison the results obtained by using AWGN channel is also included together with the main target which is frequency selective channel. For practical testing the image file (Figure 5.2) which is an artistic work of Ethiopian women with traditional dress is used. This image file is then converted to digital data as shown in Figure 5.3 below. After gray coding and QPSK modulation the resulting signal was passed through AWGN and Frequency selective fading channels which results in the following results.

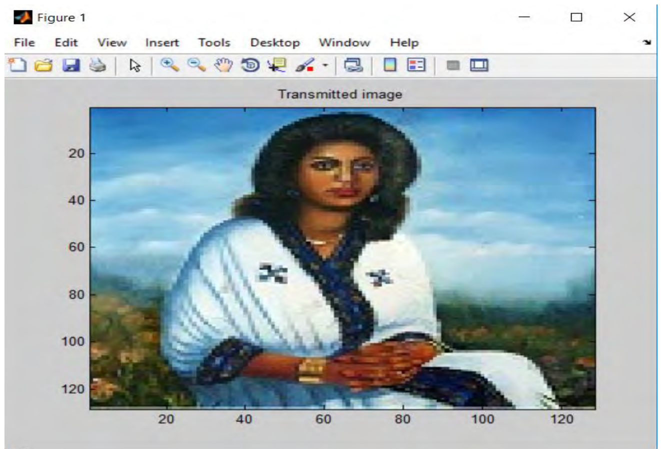

Figure 5.2: Transmitted image signal

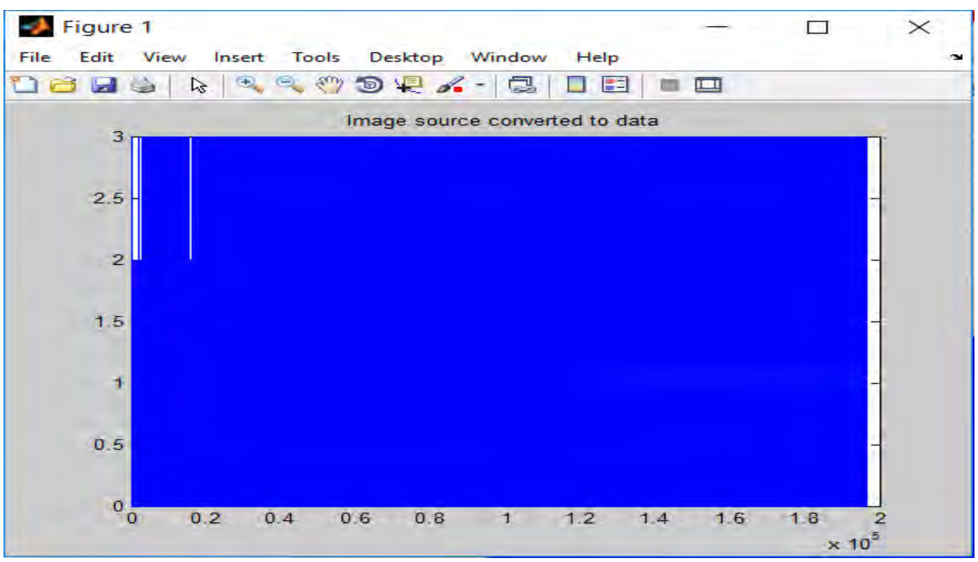

Figure 5.3: Image signal converted to data

At the transmitter and receiver filters, interpolator and decimator filter objects were created, which incorporate up sampling and down sampling, respectively, and are implemented with FIR filter. The impulse and frequency response of those filters are matched and given in Figure 5.4 below.

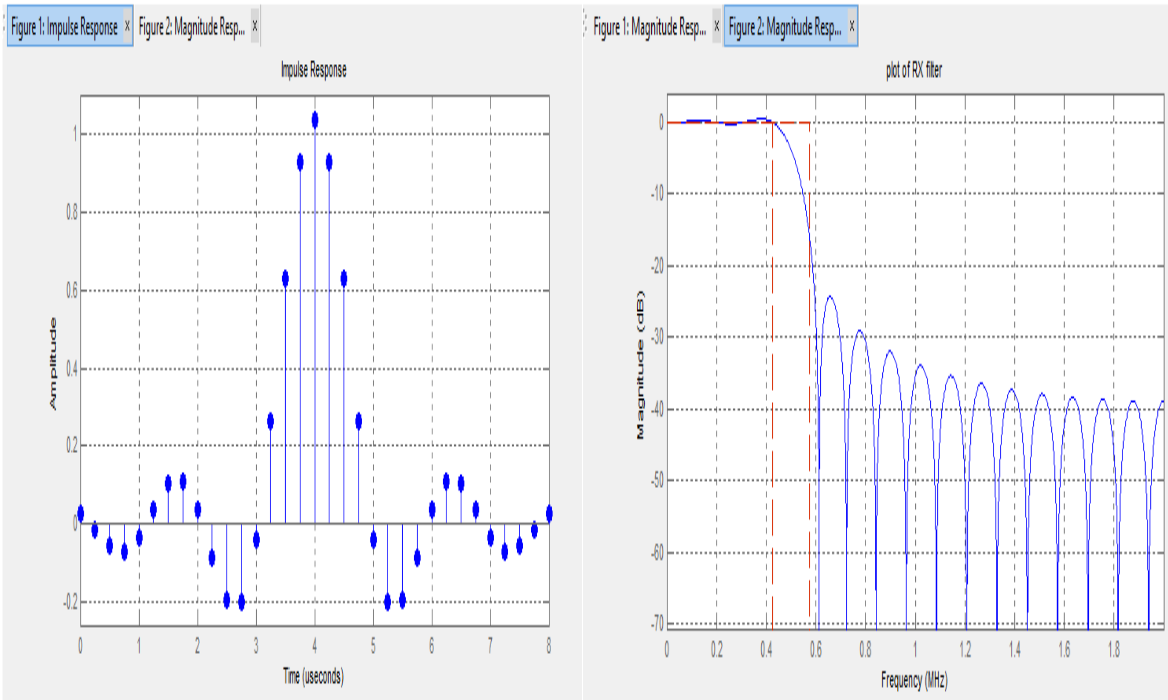

Figure 5.4: Impulse and frequency response of the pulse shaping filter

5.3.1 AWGN Channel

In this section the results obtained when the channel used for simulation is AWGN channel are presented.

5.3.1.1 BER Performance in AWGN Channel

Figure 5.5 below shows the BER performance comparison of the simulated result with the theoretical BER performance of AWGN channel for the case of QPSK modulation. As shown in the figure, the BER performance of the simulation result is closely identical to theoretical BER performance of AWGN channel. It can also be observed from this result that with just 10 dB SNR a BER performance of 10^{-5} can be achieved.

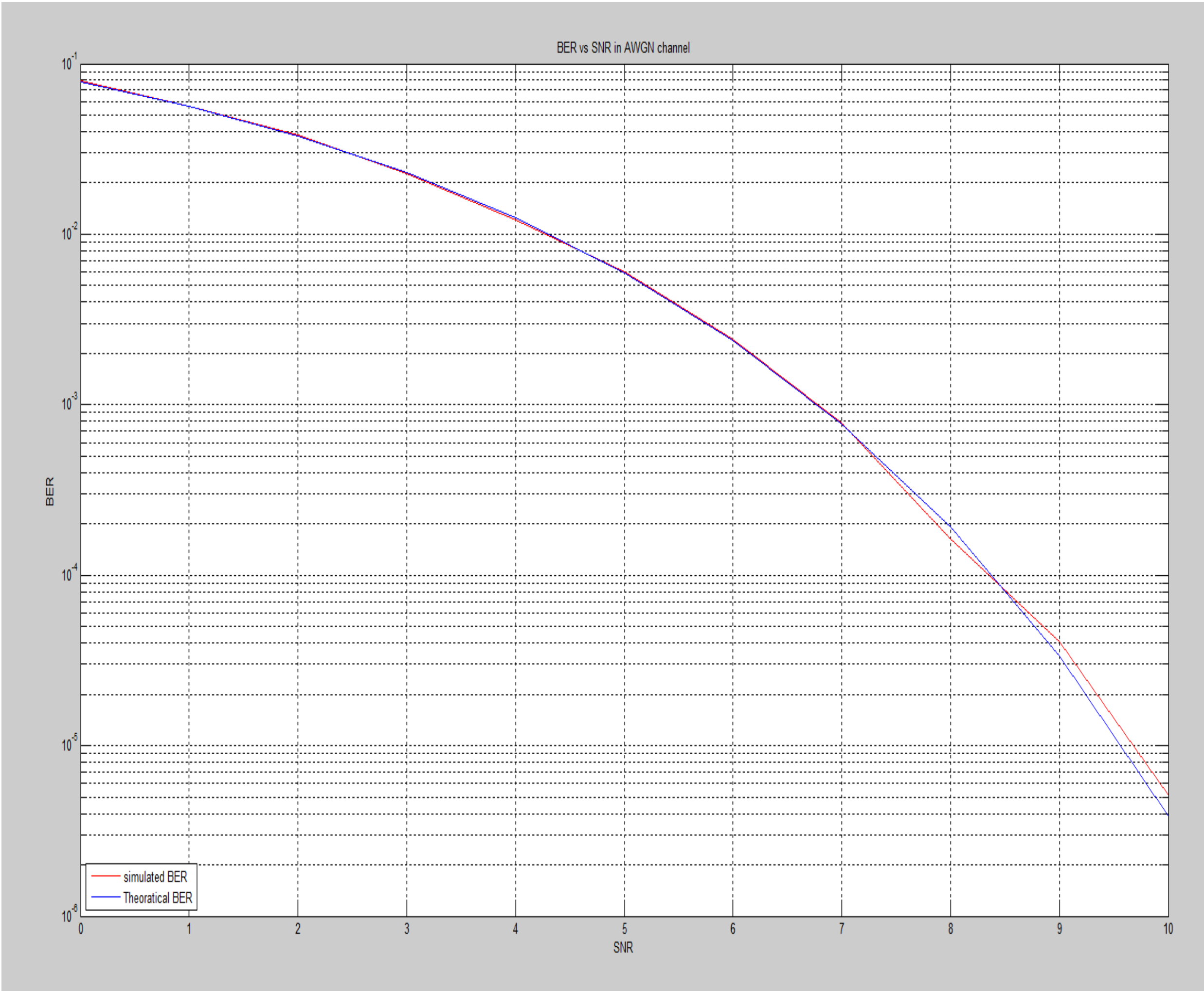

Figure 5.5: BER vs. SNR performance of AWGN channel

5.3.1.2 Image Quality of the Received Image

The next images (Figure 5.6 and 5.7), are used to show the image quality of the reception process in AWGN channel. The plots are made at two different SNR levels to meet different performance levels. In Figure 5.6, the received image is plot at 5dB SNR and in this case it is shown that there are some random noises in the image. The image quality is arguably poor for this SNR level.

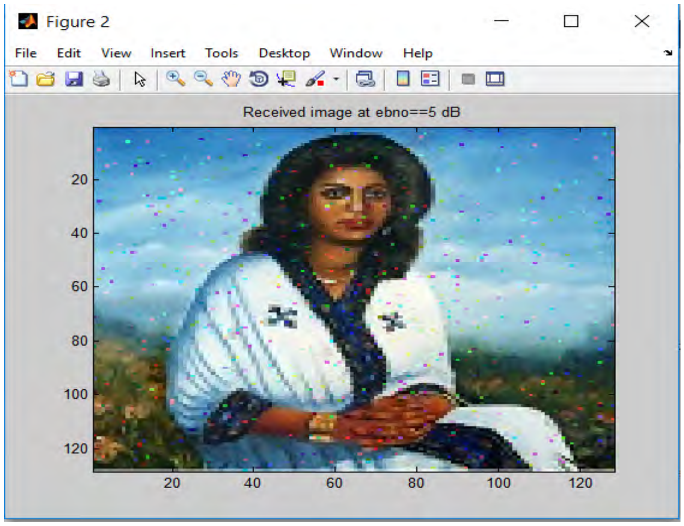

Figure 5.6: Received signal in AWGN channel at 5dB SNR

For the second case, the received image is plot at 9 dB SNR. Figure 5.7 shows the simulation result for this case and the received image quality is almost the same as the original painting.

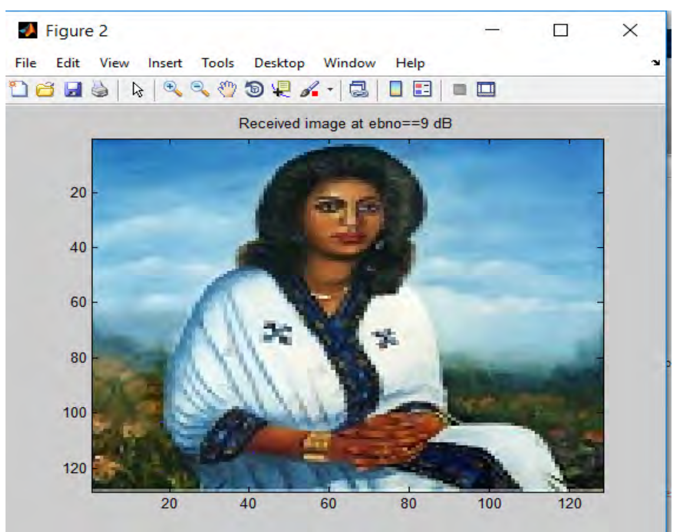

Figure 5.7: Received signal in AWGN channel at 9 dB SNR

However this type of channel is ideal and usually unrealistic in real world systems as it rarely occurs in communication system applications. It is used in this paper as a reference to compare the performance of the equalizer system to operate on the most common frequency selective fading channels.

5.3.2 Frequency Selective Fading Channel

This section presents the results obtained after generating a frequency selective fading channel and using RLS equalizer at the receiver. The simulation parameters were set according to the parameters given under Table 5.1.

5.3.2.1 Frequency Selective Fading Channel Representation

Figure 5.8 below shows the band limited impulse and frequency response of frequency selective channel used for simulation. It shows that there are 6 signal components with one signal component arriving without delay and the rest five components arriving at 0.2, 0.6, 1.6, 2.4, and 5.0 μs delays respectively. The magnitudes of each of these 6 components is set to vary randomly with time. The frequency response of this channel also shows that different frequency components exhibit different fading characteristics. However, since the maximum speed of the receiver is limited to $60 km/hr$, the signal experiences slow fading characteristics depending on the operating frequency.

Figure 5.9 also shows the visualization of those 6 multipath components. In the figure, each of the six components are shown to experience different gain characteristics. However, those components are shown to have nearly fixed gain characteristics in one symbol period. It can be noted that Figures 5.8 and 5.9 show the software implementations of TU6 channel model discussed earlier.

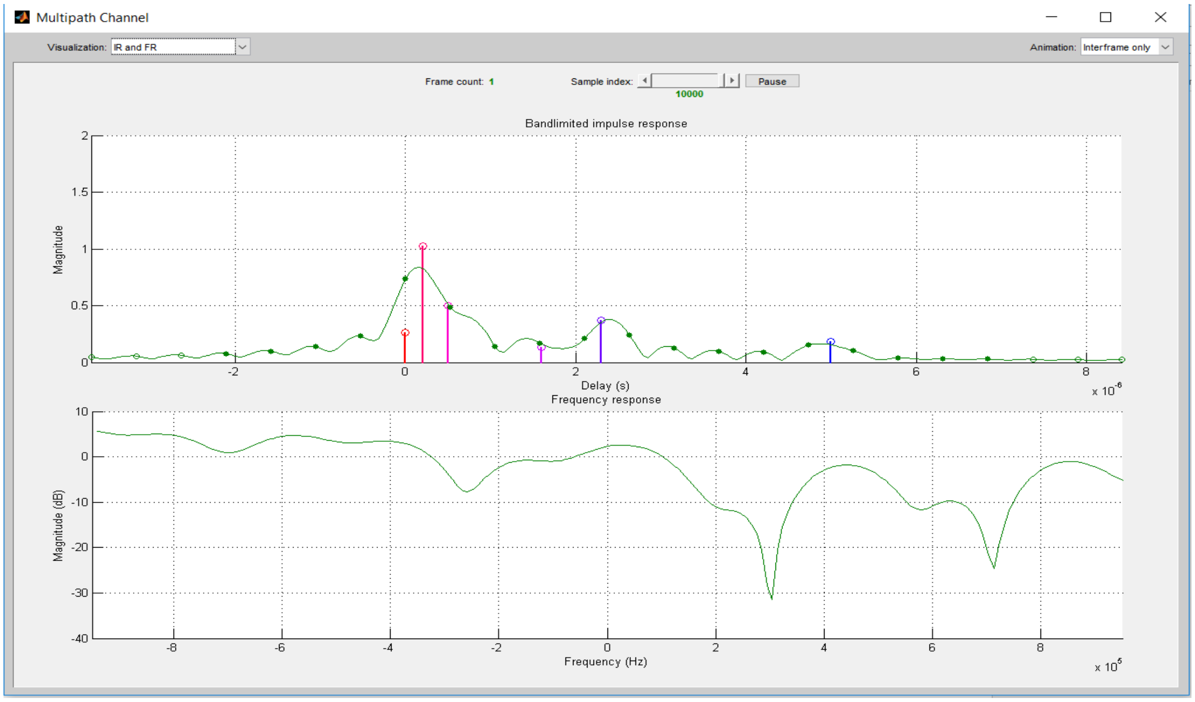

Figure 5.8: Band limited impulse response of frequency selective channel

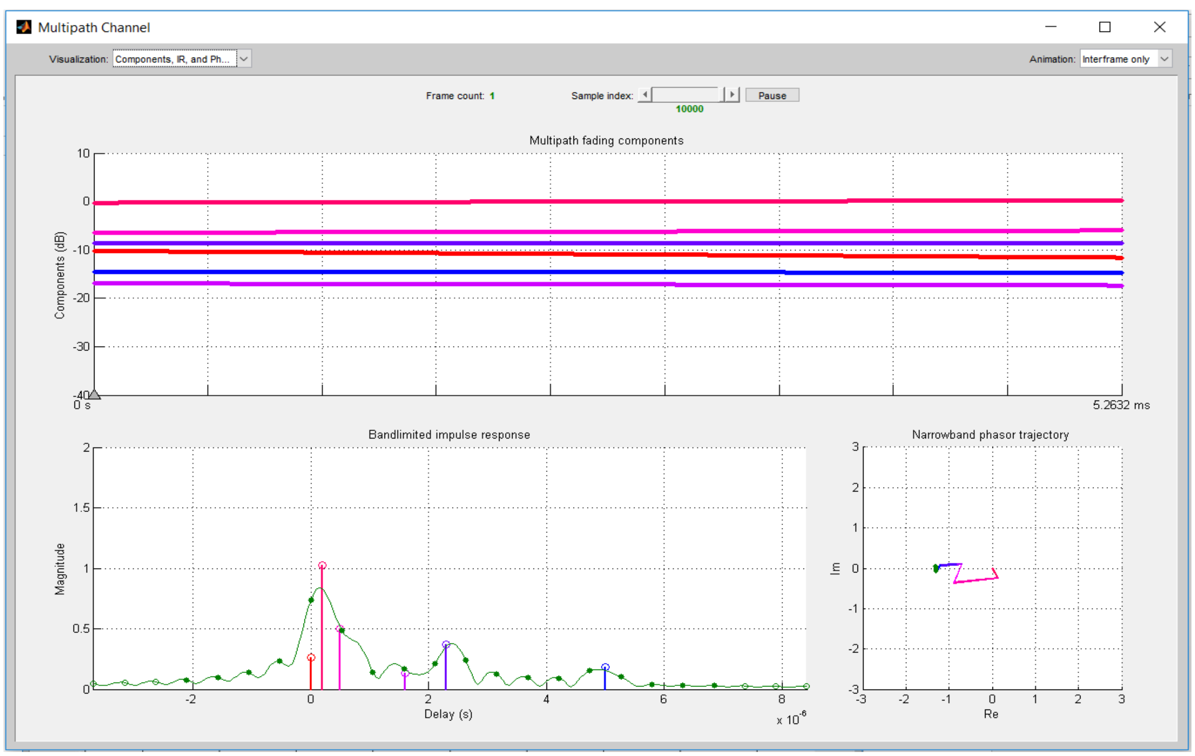

Figure 5.9: Multipath fading components under TU6 channel

5.3.2.3 BER Performance Using RLS Equalizer

Figure 5.10 shows the BER vs SNR plot of RLS algorithm by using training only mode. The figure compares the BER performance of the reception process with and without the RLS equalizer. From the result, it can be observed that the BER decreases with increasing the SNR in dB. It can also be observed that the BER performance fails to achieve 10^{-4} below 15 dB SNR and at around 15 dB it was possible to achieve this performance which is smaller than the sufficient condition for image reception which requires a BER performance less than 2×10^{-4}. This BER performance can also be further reduced to 10^{-5} by increasing the SNR to 24dB. Hence, it is also possible to use this type of equalizer for video transmission at around 18dB SNR.

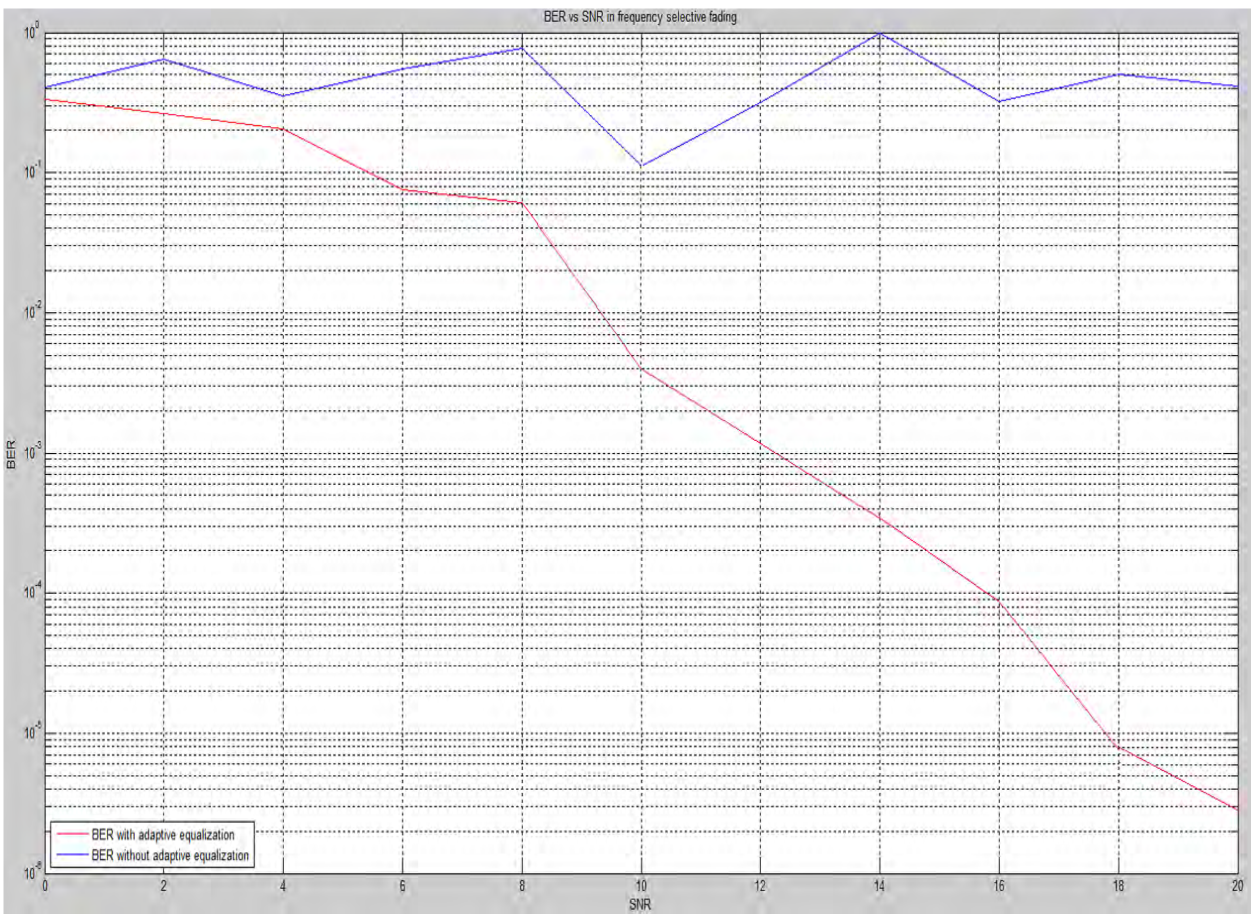

Figure 5.10: BER performance of RLS equalizer in training only mode

5.3.2.4 Constellation Plot Using RLS Equalizer

Figure 5.11 shows the constellation plot of the received signal constellation after passing the image signal in the mentioned frequency selective channel at 15dB SNR value. The first column in the figure consists of the received constellation before and after the RLS equalizer. Here the red circles are used to represent wrongly received bits while blue ones are used to represent correctly received bits. From the first figure it is shown that the BER performance before equalization was 0.94 which means out of the transmitted 100 bits 94 of them were received wrongly. This poor performance was the result of ISI caused by frequency selective channel used for transmission.

The second constellation plot shows the equalized constellation plot after passing the received constellation through RLS equalizer. The equalizer is an 8-tap RLS equalizer whose weights are plotted under equalizer weights title. The training method used in this case was training only mode. In this plot the equalizer weights are complex valued numbers in which blue lines are used to represent their real values while magenta colored lines are used to represent the imaginary values of each equalizer weights. The last plot shows the squared error magnitude which is as small as less than -5dB.

Here it is shown that the original QPSK constellation is recovered successfully after passing the QPSK demodulated signal through RLS equalizer. Its BER performance is shown to be 0.00014 which is small enough for image transmission whose standard BER performance requirement is $BER < 2 \times 10^{-4}$.

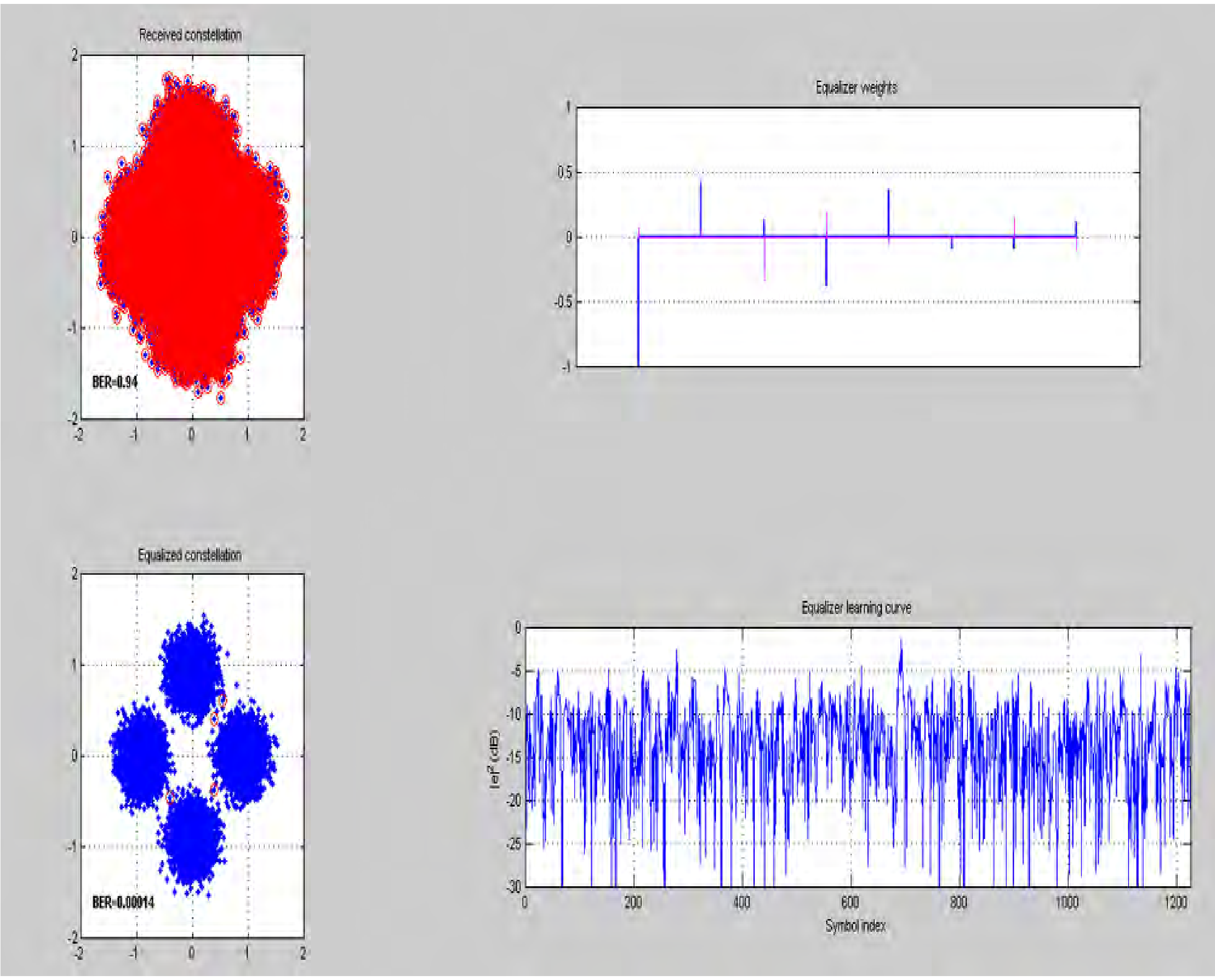

Figure 5.11: Constellation plot of RLS equalizer at 15 dB SNR

5.3.2.5 Image Quality Comparison

Figure 5.12 and 5.13 show the images received before and after equalization respectively. As shown in Figure 5.13, the received image before equalization is very erroneous and difficult to identify. The result is expected as the image was received while the channel BER is 0.94. However it was possible to treat this signal to recover the original transmitted image successfully by using RLS equalizer. Figure 5.13 shows the equalized image after passing the received signal through RLS equalizer. It can be observed that the equalized image in this figure is almost the same as the original transmitted image.

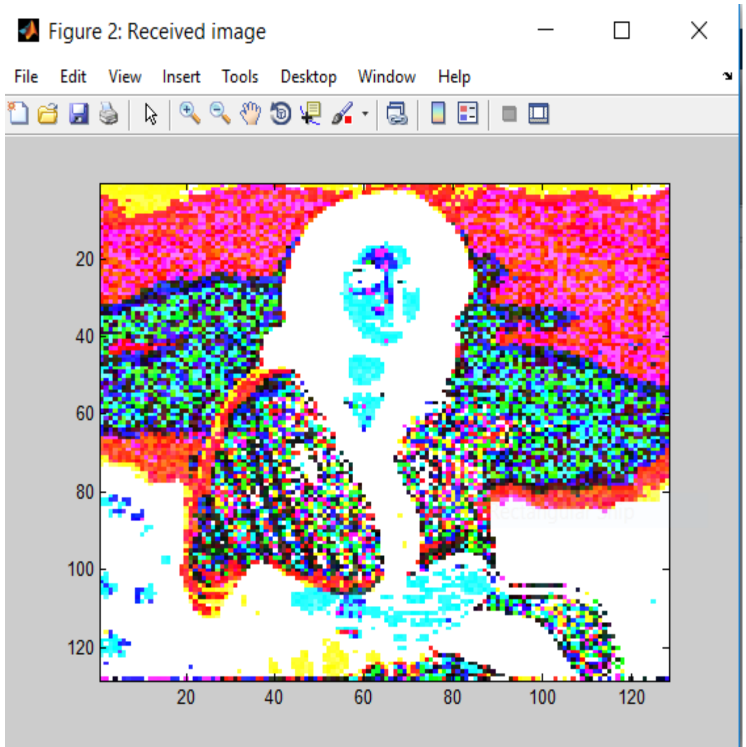

Figure 5.12: Received image under frequency selective channel before equalization

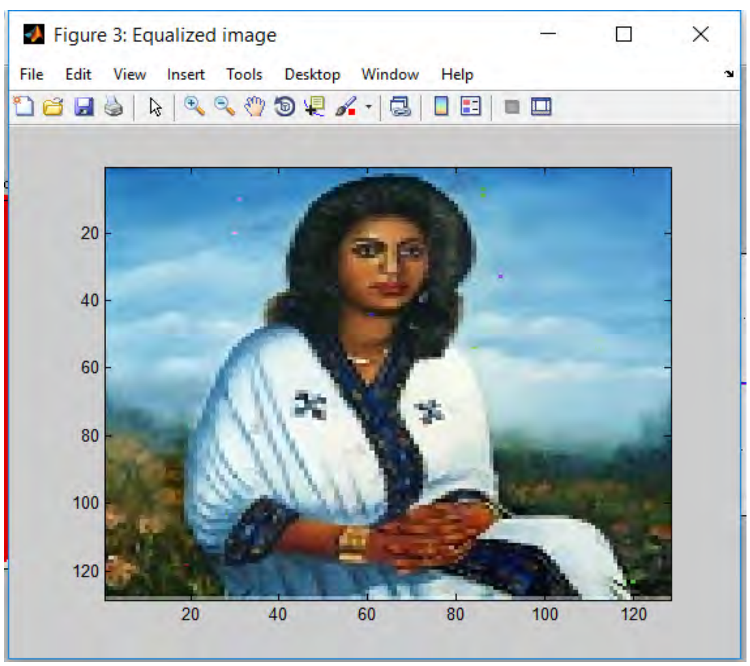

Figure 5.13: Received image after equalization at 15dB

5.3.2.6 Performance of RLS Equalizer Using Decision Directed Training Mode

The results so far were obtained by using training only mode and the next images show the performance of RLS equalizer using decision directed training mode. It can be observed that the performance of the equalizer is improved when compared to the training only mode. Observing at the constellation plot, the squared error magnitude is nearly similar for the first few symbol indexes in both training only and decision directed training methods. However, after few symbol indexes, the error magnitude in decision directed training mode is much smaller than error magnitude in training only mode. This results in improvement in the performance of the equalizer in decision directed training mode.

With similar parameters used for training only mode the following results were obtained in decision directed training mode at 15dB SNR. A BER performance of 2.3×10^{-5} was achieved at 15dB SNR. This BER performance is small enough for data and video transmission which requires less than 7×10^{-5} BER as a quality of service.

Figures $(5.14 - 5.17)$ show the constellation plot, BER vs SNR and image quality comparisons before and after the RLS equalizer in the decision directed training mode. The results show that the performances are improved when compared to training only equalizer.

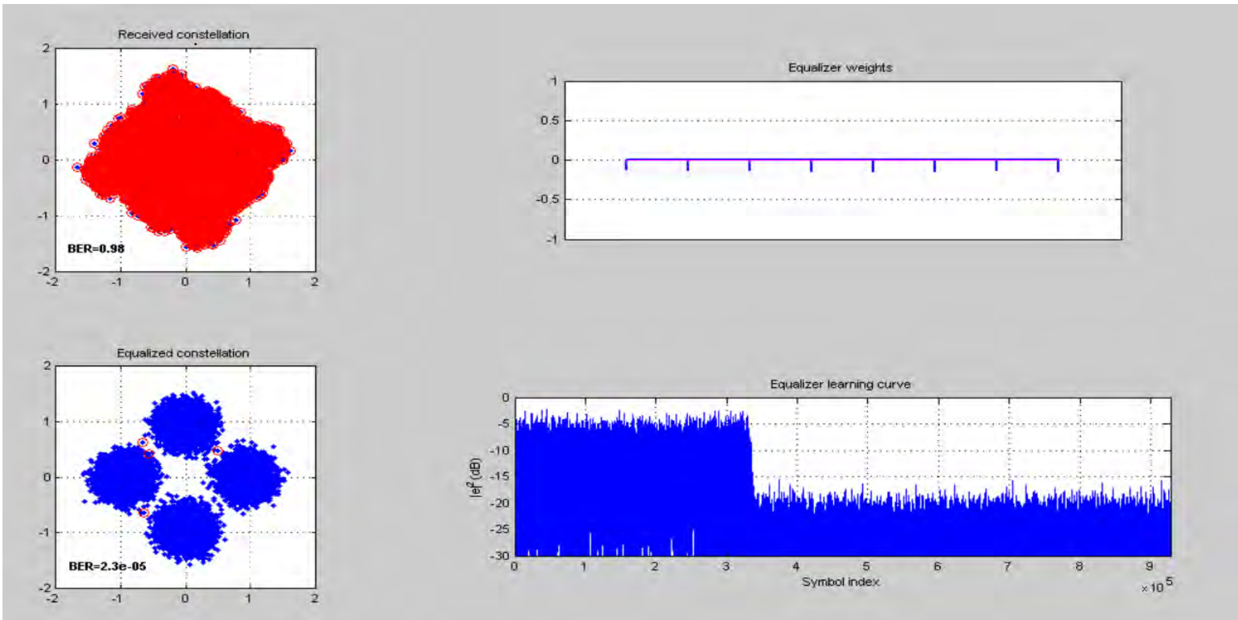

Figure 5.14: Constellation plot of RLS equalizer using decision directed training mode

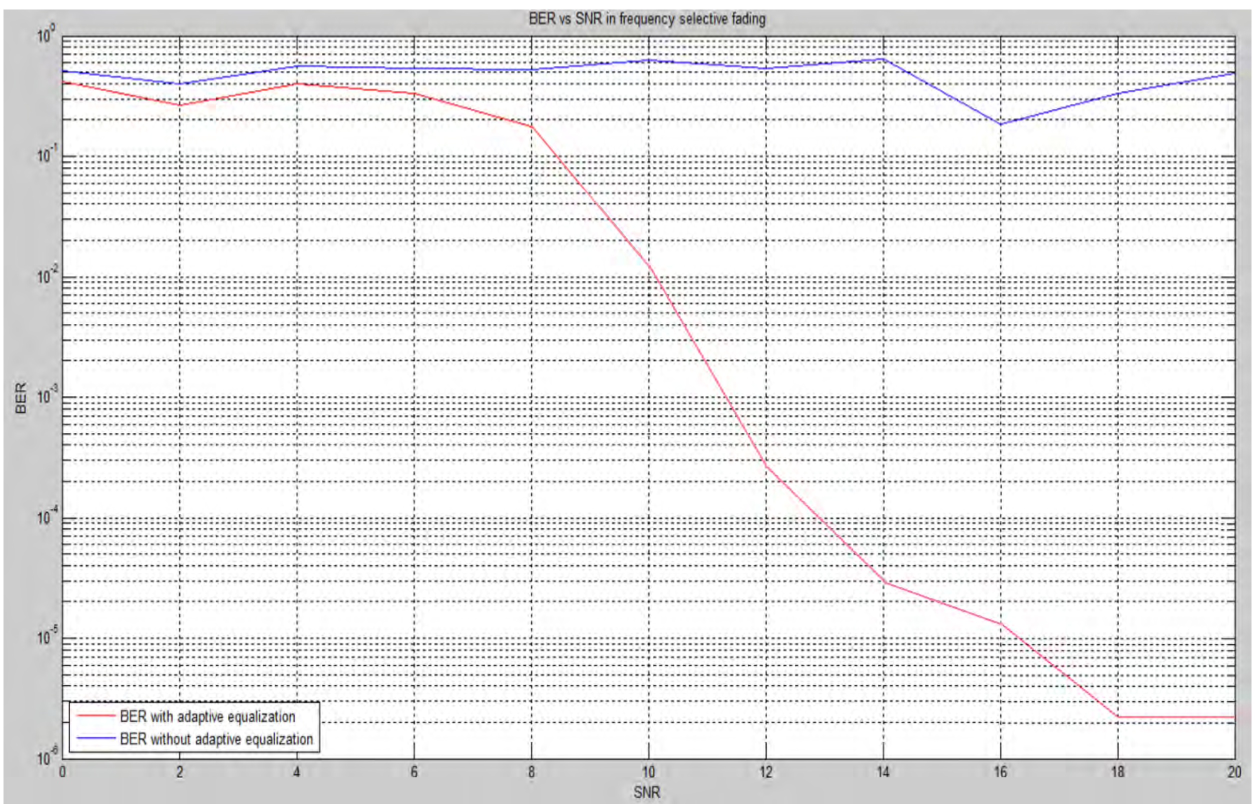

Figure 5.15: BER performance of RLS equalizer in decision directed mode

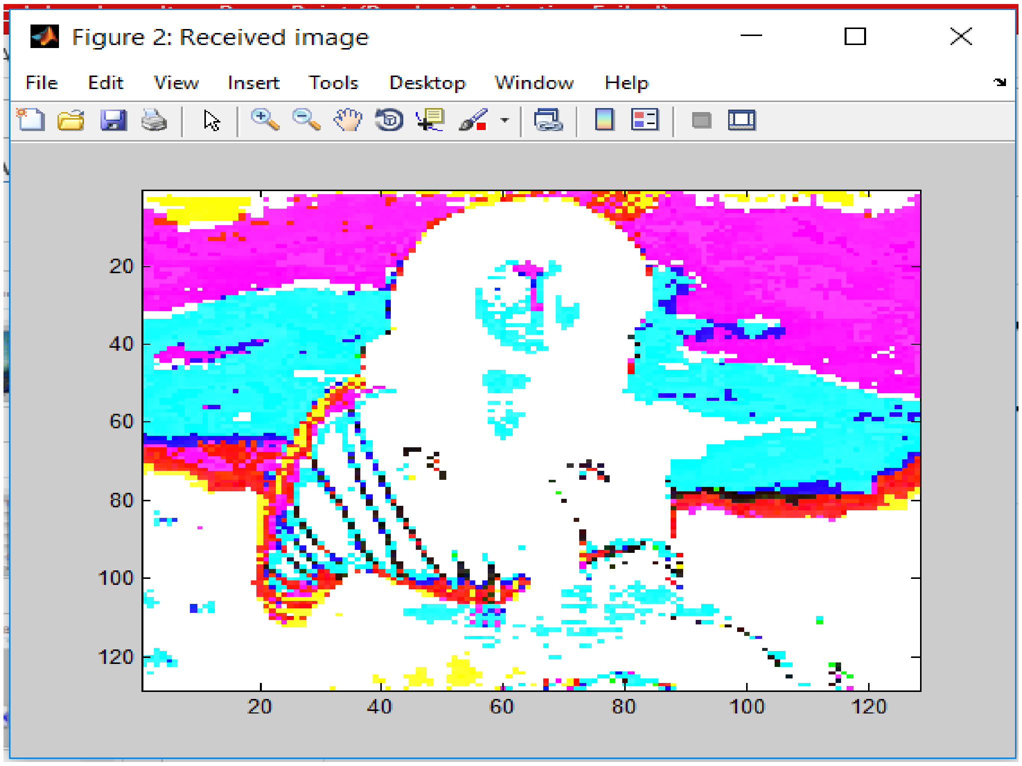

Figure 5.16: Received image before equalization

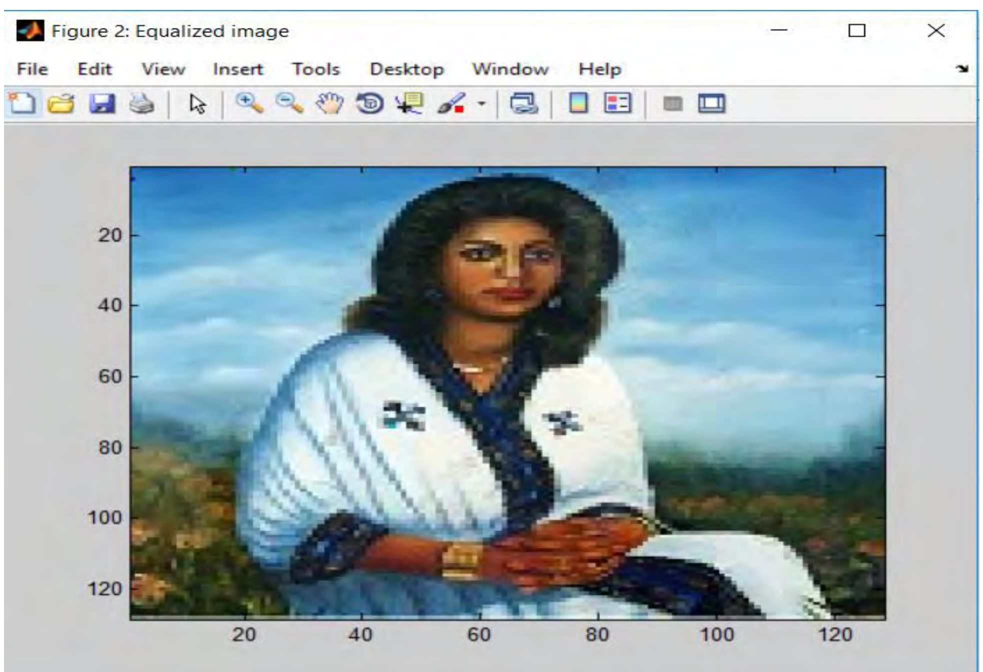

Figure 5.17: Equalized image after equalization in decision directed mode

5.4 Results Summary

In both training only and decision directed training modes, the original image signal which was corrupted by ISI in frequency selective channel was recovered successfully. In training mode the BER performance of the RLS equalizer at the specified parameters was 1.4×10^{-4} . This performance is sufficient for voice, audio and image transmission since BER performance requirement is BER less than 2×10^{-4}. However for video transmission the BER performance requires a BER value less than 7×10^{-5} and this technique may fail to recover the original signal successfully. In this case decision directed training mode can be used to improve the performance of the RLS equalizer or increase the power up to 20dB in training only mode.

From those results the original image signal was recovered without the need of equalizers in AWGN channels at around 10dB SNR. On the other hand, when the channel is frequency selective RLS equalizer was required to reverse the effect of the dispersive channel and an extra 5dB SNR to recover the corrupted image successfully. The performances of two types of training methods was also investigated. From the results it was shown that the decision directed training method performing better than the training only method. However, the later one is less complex in terms of computational loads and good enough to be used for voice, audio and image transmissions in terms of BER performance at 15dB SNR.

Chapter Six

Conclusions and Recommendations

6.1 Conclusions

The main objective of this thesis work was to study and analyze the performances of selected adaptive equalizers that can be used in broadcast channels. In general those equalizers were classified in to non-blind, blind and semi-blind equalizers based on their approach to estimate the behavior of the channel used for communication. From those categories non-blind equalizers perform better than both blind and semi-blind methods at the expense of bandwidth efficiency due to the transmission of overhead training sequence. Because of their performance non-blind equalizers were chosen to be the main focuses of this thesis with their training sequence length limited to 8% of the total transmitted bits to improve its bandwidth efficiency.

From non-blind methods, ZF, MMSE, LMS, RLS, DFE and MLSE equalizers were reviewed in this thesis and their performances were compared based on the criteria of computational complexity, numerical stability, convergence speed to obtain the optimal filter weight and BER minimization performance. Taking all the trade-offs between those metrics, RLS algorithm based linear equalizer was found to be appropriate technique and it was implemented in MATLAB software for simulation. The simulation setup was based on QPSK modulation. AWGN and frequency selective channel (modeled as TU6 channel) were also considered for performance comparisons. In AWGN case the receiver was implemented without the use of equalizers while RLS equalizer was used in frequency selective case. Also the performance of RLS equalizer based on training only and decision directed training methods was investigated in simulation.

From the simulation results, the RLS equalizer in frequency selective channel needs extra 5dB SNR compared to AWGN channel to recover corrupted image signal successfully which requires a BER performance of less than 2×10^{-4}. Also decision directed training method was found to perform better than the training only method in TU6 channel by achieving a BER performance of 2.3×10^{-5} at 15dB SNR. This BER performance is sufficient for video transmissions which requires a BER performance of less than 7×10^{-5}. Based on the study and results obtained, implementation of RLS equalizer with decision directed training mode is recommended for the sponsor industry (INSA).

6.2 Recommendations

In this thesis, QPSK modulation was used to test the effect of different channels to the received data. So, only the channel phase information was estimated and equalized in the mitigation process. In future works more modulation techniques could be included such as ASK and QAM with different modulation orders. In such cases, estimation of both the channel phase information and amplitude information will be included.

RLS algorithm based linear equalizer was also used in simulation works in this thesis with the assumption that there is no deep fading in the pass-band. However, linear equalizers do not usually perform well on channels which have deep spectral nulls in the pass-band. For such cases, the work can be improved by adding non-linear equalizers like DFE and MLSE. Also, all of the implementations are made in MATLAB software at present. In future works, the simulation model can be integrated into GNU radio with USRP hardware support, which will give a practical environment to test wireless communication system simulations and FPGA implementations could also be included for physical implementations.

References

[1] L. M. Jimenez, "Channel Estimation Architechures for Mobile Reception in Emerging DVB Standards," Mondragon University, Mondragon, May 2012.

[2] G. J. Miao, Signal Processing in Digital Communications, 1st ed., Norwood: Artech House, Inc., 2007.

[3] K. Wesolowski, Introduction to Digital Communication Systems, 1st ed., Warszawa: John Wiley and Sons Ltd., 2009.

[4] J. G. Proakis, Digital Communication Systems, 4th ed.

[5] S. J.Orfandis, Optimal signal Processing an Introduction, 2nd ed., New York: McGraw-Hill publishing company, 2007.

[6] S. Jalali, "Wireless Channel Equalization in Digital Communication Systems," CGU Theses & Dissertations, Claremont Graduate University, 2012.

[7] Kalyan Chakravarthy Talluri & Jaswini Reddy Potuganuma, "Semi Blind Fractionally Spaced Equalizers," Blekinge Institute of Technology, December 2010.

[8] R. Beutler, The Digital Dividend of Terrestrial Broadcasting, New York, USA: Springer Science+Business Media, 2012.

[9] Mudit Shukla, G. R. Mishra, O. P. Singh, Sachin Kumar & Kamal Ahmed, "Parametric Optimization and Analysis of Adaptive Equalization Algorithms for Noisy Speech signals," IOSR-JEEE, Amity University, India, 2013.

[10] S. Das, "Mathematical Methods for Wirless Channel Estimation and Equalization," Wein University, August, 2009.

[11] P. Hakala, "Comparison of Channel Models for Evaluating the Performance of Mobile Broadcasting Systems," DTV Group, University of Turku, St. Petersburg, 2007.

[12] A. Goldsmith, Wireless communications, New York: Cambridge University Press, 2005.

[13] T. S. Rappaport, Wireless Communication Principle and Practice, 2nd ed.

[14] Franz Hlawatsch & Gerald Matz, Wireless Communications over Rapidly Time-Varying Channels, Oxford, UK: Elsevier Ltd., 2011.

[15] J. S. Seybold, Introduction to RF Propagation, Hoboken, New Jersey: John wiley & Sons, INC., 2005.

[16] Ke-Lin Du & M. N. Swamy, Wireless Communication Systems, New York: Cambridge University press, 2010.

[17] John G. Proakis & Masoud Salhi, Digital communications, 5th ed., New York: McGraw-Hill, 2008.

[18] Edward A. Lee & David G. Messerschmitt, Digital Communication, Dordrecht, Netherlands: Kluwer Acadamic Publishers, 1988.

[19] D. Tse, Fundamentals of Wireless Communication, California: Cambridge University Press, 2004.

[20] M. Patzold, Mobile Radio Channels, 2nd ed., University of Agder, Norway: John Wiley & Sons, Ltd., Publication, 2012.

[21] M. Patzold, Mobile Fading channels, Agder University college, Grimstad, Norway: John Wiley & Sons, Ltd., 2002.

[22] COST207, Digital Land Mobile Radio Communications, Luxembourg: Commission of the Europian Communities, 1989.

[23] Y. Akaiwa, Introduction to Digital Mobile Communication, 2nd ed., Hoboken, New Jersey: John Wiley & Sons, Inc., 2015.

[24] Prachi Sharma, Piush Gupta & Pradeep Kumar Singh, "Performance Comparison of ZF, LMS and RLS Algorithms for Linear Adaptive Equalizer," *AEEE,* vol. 4, no. 2, pp. 587-592, 2014.

[25] N. Charaya, "Performance Analysis of Adaptive Channel Equalizer Using Different Algorithms," *IJRRA,* vol. 3, no. 2, pp. 28-31, June 2016.

[26] Mohapatra Ku. Pradyumna, Siba Prasad Panigrahi & Jibanananda Mishra, "Improved Adaptive Bit Error Rate Performance," *IJAIEM,* vol. 2, no. 9, pp. 275-282, September 2013.

[27] Ruyet Le Didier & Mylene Pischella, Digital Communications 2, Hoboken, USA: John Wiley & Sons, Inc., 2015.

[28] M. H. Hayes, Statistical Signal Processing and Modelling, 3rd ed., Georgia Institute of Technology, 1996.

[29] Arthur A. Giordano & Allen H. Levesque, Modeling Of Digital Communication Systems Using Simulink, Hoboken, New Jersey: John Wiley & Sons, Inc. , 2015.

[30] Branko Kovacevic, Zoran Banjac & Milan Milosavljevic, Adaptive Digital Filters, Belgrade: Academic Mind, 2013.

[31] Jay Prakash Vijay & Nitin Kumar Sharma, "Performance Analysis of RLS over LMS Algorithm for MSE in Adaptive Filters," *IJTEEE,* vol. 2, no. 4, pp. 40-44, 2014.

[32] O. Hafenden, "DVB-T2: The Common Simulation Platform," British Broadcasting Corporate, May 2011.

[33] C. R. Nokes, "DVB-T2 Receiver Buffer Model: Theory and Practice," BBC R&D, July 2012.

[34] E. Ahmed, W. Aziz, G. Abbas, S. Saleem & Q. Islam, "Channel Estimation for OFDM System using Training Sequence Algorithms," *AEES,* vol. 1, no. 3, 2012.

[35] S. Haykin, adaptive Filter Theory, 3rd ed., 2002.

[36] Gunjan Verma, Prof. Jaspal Bagga, "Performance Analysis of Equalizer Techniques for Modulated Signals," *IJERA,* vol. 3, no. 4, pp. 1191-1195, 2013.

[37] K. Gentile, "The Care and Feeding of Digital Pulse-Shaping Filters," RF Design, Greensboro, 2002.

[38] Nuzhat Tasneem Awon & Md. Mizanur Rahman, "Effect of AWGN & Fading Channels on BER perfromance of a WiMAX communication system," IJCSIS, Rajshahi, Bangladesh, 2012.

[39] A. F. Molisch, Wireless Communications, 2nd ed., California, USA: John Wiley & Sons Ltd,, 2011.

[40] Farheen Ali, Paresh Rawat & Sunil Malvia, "Comparative Analysis and Survey of LMS and RLS Adaptive Algorithms," *IJCA,* vol. 161, March 2017.

[41] Seema Paliwal, Dilpreet Kaur Grover & Jyoti Krayla, "Comparison of Linear and Non-linear Equalizers Using the Matlab," New York, USA, 2016.

[42] G. Bottemley, Channel Equalization for Wireless Communications, Hoboken, New Jersey: John Wiley and Sons Ltd, 2011.

[43] H. Kim, Wireless Communication Systems Design, Chichester, UK: John wiley & Sons, Ltd, 2015.

[44] Amandeep Singh Sappal & Garima Malik, "Adaptive Equalization Algorithms," *IJACSA*, vol. II, March, 2011.

[45] N. D. Sidiropoulos, Communications and Radar Signal Processing, 1st ed., Waltham, USA: Elsevier Ltd., 2014.